NTNU – Trondheim
Norwegian University of
Science and Technology

Numerical Modeling of Cyclic Loading on Clay

Christofer Klevsjø

Civil and Environmental Engineering
Submission date: June 2014
Supervisor: Gustav Grimstad, BAT

Norwegian University of Science and Technology
Department of Civil and Transport Engineering

NORWEGIAN UNIVERSITY OF SCIENCE AND TECHNOLOGY
DEPARTMENT OF CIVIL AND TRANSPORT ENGINEERING

Report Title:	Date: June 10, 2014			
Numerical Modeling of Cyclic Loading on Clay	Number of pages (incl. appendices): 143 + cover			
	Master Thesis	**X**	Project Work	
Name: Christofer Klevsjø				
Professor in charge/supervisor: Prof. Gustav Grimstad				

Abstract:

Soil`s behavior, when subjected to cyclic loading, may often be reduced stiffness giving large deformations. For undrained conditions a possible pore pressure build-up will reduce the capacity even further. This may affect the design of foundations and the stability of slopes.

Undrained cyclic response of clay has been simulated by an Iwan model combining several elasto-plastic soil models coupled in parallel. Each of these models was assigned with a unique set of parameters. The soil behavior is described by the Cam Clay Model, with a degradation term implemented. The cyclic model is independent of the frequency of the applied load.

Seven triaxial tests have been conducted, where five of these were cyclic tests with different cyclic amplitudes. High friction forces were found to disturb the quality of the cyclic tests. In addition one creep test, and one shear test was conducted.

The results from the cyclic simulation is totally dependent on the number and values of the parameters used. The interaction between them will also influence the results. Manually determination of the parameters needed are a time-consuming process. A recommended solution to improve the model is to find an automatic method where the parameters could be determined from a representative cyclic triaxial test.

Based on the most common results from the triaxial simulations, a realistic pore pressure build-up may be modeled. Hysteresis in the soil will also be accounted for. However, low accumulation of plastic strains and only a slight change in stiffness resulted in approximate identical hysteresis loops calculated for each cycle. The reason for this is most likely that the right value, number and interaction between the included parameters have to be found. There are some unsolved issues regarding modeling of the permanent strain that have to further be evaluated. By solving these problems, the presented method for modeling undrained cyclic loading on clay is likely to be representative for the general trend of the soil`s behavior.

Keywords:

1. cyclic modeling	2. cyclic triaxial test	3. cam clay model
4. iwan model	5. degradation	

Preface

This master thesis was written at the Norwegian University of Science and Technology, NTNU, in Trondheim during the spring semester of 2014. By completing this thesis I will obtain a Master of Science degree in Civil and Environmental Engineering, with a specialization in Geotechnical Engineering. My supervisor through this semester has been Professor Gustav Grimstad at NTNU.

The subject for this thesis was brought up to me by Professor Grimstad. He had on earlier stage stated a process for modeling cyclic behavior of soil. This process has been modeled in a finite element program. Triaxial tests has also been conducted to give a basis for the simulated results.

This last semester I have learned both practical and theoretical knowledge regarding soil behavior. Still I would like to emphasize the learning outcome from the laboratory testing. This has given me insight and knowledge that will be useful in further geotechnical work. Completing this thesis marks the end of a five years period as student at NTNU. I know that the new relations and the way of thinking obtained from this period will affect me on a daily basis hereafter.

Acknowledgment

Credit and acknowledgments have to be awarded to Professor Gustav Grimstad. The basis for the thesis was done based on his thoughts and insight into this subject. Throughout this semester he has provided educational sessions and brought up new ideas for the development of the model.

The triaxial testing was done with a close dialog with divisional engineer Per Østensen and research assistant Helene A. Kornbrekke. The quality of the tests was highly improved by the help from these two. The PhD candidates Jon A. Rønningen and Hilde A. Nøst have been helpful and patient in the process of finding numerical errors in the coding.

Other people of the staff at the Geotechnical Division at NTNU have also contributed in varying extent. Either by a quick and informative comment or by longer conversations.

Trondheim – June 10, 2014

Christofer Klevsjø

Summary and Conclusions

Earthquakes, traffic, wind etc. may cause vibrations in the soil. For the design of foundations and the stability of slopes this can be an important factor. The response of the soil, subjected to this type of loading, may often be a reduced stiffness and capacity and large deformations.

On the marked today, there is no software that is able to accurately model the effect from cyclic loading on clay. One way to model undrained cyclic behavior is to combine, by an Iwan model, several elasto-plastic material models in parallel. This enables the hysteresis effect and the pore pressure build-up to be accounted for. An advantage of using Iwan models is that all parameters included are associated with the soil models used. The model is independent of mass and damping, which implies that the model is not dependent of frequency of the applied load. In this thesis the soil behavior is described by the Cam Clay Model, with a degradation term implemented.

Seven triaxial tests have been conducted. Five of these were cyclic tests, with different cyclic amplitudes. One was done as a creep test, and one as a shear test. High friction forces were found to disturb the quality of the cyclic tests. The average pore pressure build-up and vertical strain are found to be representative. Results related to the triaxial testing device are presented for improvement of further testing.

Based on the general trend from the triaxial simulations a realistic pore pressure build-up may be modeled, hysteresis in the soil will also be ac-

counted for. However low accumulation of plastic strains and only a slight change in stiffness resulted in approximate identical hysteresis loops calculated for each cycle. The reason for this is most likely that the right value, number and interaction between the included parameters have to be found. There are some unsolved issues regarding modeling of the permanent strain that have to be further evaluated. By solving these problems, the presented method for modeling undrained cyclic loading on clay is likely to be representative for the general trend of the soil's behavior.

A possibility to obtain the parameters need for an accurate simulation of the cyclic behavior of the soil is to obtain the values from a cyclic triaxial test preformed on a representative soil sample. A mathematical algorithm could be used to find the best match between the cyclic test and the modeled result. The values obtained could be verified by back calculating another cyclic test. This solution requires triaxial testing of high quality. Modification to the triaxial device, used in this thesis, should be done before any more testing is conducted.

Contents

Preface **v**

Abstract **vii**

Contents **ix**

1 Introduction **1**
1.1 Background 1
1.1.1 Problem formulation 2
1.1.2 What remains to be done 2
1.1.3 Literature survey 2
1.2 Objective and Scope 3
1.3 Limitations 3
1.4 Approach 4
1.5 Outline of Thesis 4

2 Theory **7**
2.1 Elasto- Plasticity 7
2.1.1 Elasticity 7
2.1.2 Plasticity 8
2.2 Linear Elastic Perfect Plastic Soil Model 9
2.3 The Cam Clay Model 10
2.3.1 Undrained loading 13
2.3.2 Softening 16

2.4 Finite Element Method 17

3 Cyclic Loading **19**
3.1 Stresses and Strains 19
3.2 Properties of Soil 21
3.2.1 Degradation 21
3.2.2 Hysteresis effect and damping ratio 22
3.3 Modeling the Hysteresis Effect 22
3.3.1 Iwan models 23

4 Modeling Cyclic Soil Behavior using FEM **27**
4.1 User-Defined Soil Models in PLAXIS 27
4.1.1 Iwan model in PLAXIS 28
4.1.2 Distribution of initial stresses 29
4.1.3 Representation of the soil 31
4.2 Modeling Soil Response from Cyclic Loading 32
4.2.1 Pore pressure build-up 33
4.2.2 Hysteresis effect 34

5 Triaxial Test **37**
5.1 Test Procedure 37
5.1.1 Installation 37
5.1.2 Consolidation 37
5.1.3 Loading/ failure 38
5.1.4 Sample disturbance 38
5.1.5 Back pressure 39
5.2 Test Device Used 40

6 Results from Triaxial Tests **43**
6.1 Measured Pore Pressure 43
6.2 Friction 44
6.2.1 Interaction load rod and triaxial cell 44
6.2.2 Further evaluation 45
6.2.3 Conclusion 46

6.3 Creep Deformations under Cyclic Loading 47
6.3.1 Results 48
6.3.2 Conclusion 49
6.4 Effect of Degradation 49
6.5 Undrained Cyclic Shear Strength 50
6.5.1 Result 51
6.5.2 Conclusion 52

7 Results from Cyclic Modeling **53**
7.1 Validation and Evaluation of User-Defined Soil Models . . . 53
7.1.1 Triaxial shear test 53
7.1.2 Cyclic triaxial test 55
7.2 Further Evaluation of the Cyclic Results 59
7.2.1 Methods of solution 59
7.2.2 Results 60
7.2.3 Conclusion 62

8 Analysis & Discussion **63**
8.1 Numerical Modeling of Cyclic Behavior 63
8.1.1 Pore pressure 64
8.1.2 Hysteresis 64
8.1.3 Accumulated strain and change in stiffness 65
8.2 Triaxial Tests 66
8.2.1 Modifications 67
8.2.2 Corrected area 68
8.3 Improvements 69

9 Conclusions and Recommendations for Further Work **71**
9.1 Summary and Conclusions 71
9.2 Further Work 72

Bibliography **74**

List of Figures **74**

List of Tables **76**

List of Symbols & Abbreviations **79**

A Text of Thesis **83**

B Triaxial Test Results **87**
B.1 Overview of the triaxial results 87
B.1.1 Presentation of the Test Results 88
B.2 Stjørdal: Depth 10,6 meter 90
B.3 Stjørdal: Depth 10,7 meter 92
B.4 Stjørdal: Depth 11,1 meter 94
B.5 Stjørdal: Depth 11,2 meter 96
B.6 Stjørdal: Depth 11,4 meter 98
B.7 Stjørdal: Depth 11,5 meter 100
B.8 Stjørdal: Depth 11,6 meter 102

C Cyclic Strain and Stress Development **105**
C.1 Stjørdal: Depth 11,2 meter 106
C.2 Stjørdal: Depth 11,5 meter 107
C.3 Stjørdal: Depth 11,6 meter 108

D Validation **109**
D.1 Triaxial Shear Test 109
D.1.1 Cam Clay Model w/ Degradation 110
D.1.2 Multi Parameter Script 111
D.1.3 Hand calculations 112
D.2 Cyclic Triaxial Test 114
D.2.1 Model 114
D.2.2 Further evaluation of cyclic results 114

E User Manual MPS **117**
E.1 Modifications 117
E.2 Software 119

F Fortran Source Code **121**
F.1 Iwan model, parallel coupling 121
F.2 Subroutines 127
F.2.1 Parameters 127
F.2.2 Stress distribution 128

1. Introduction

Cyclic loading may be a critical factor in the design of the foundation of structures and stability of slopes. Cyclic loading has a tendency to decrease stiffness and strength of the soil. Even though the structure is subjected to repeated loading considerably less than the maximum static capacity large deformations may occur.

A commonly used method, to design for a cyclic load history where the shear stress varies with time, is to estimate an equivalent number of cycles with a representative maximum shear stress. A cyclic triaxial test is then conducted on a soil specimen to determine the cyclic capacity of the soil Andersen (2009).

On the marked today, there is no software that is able to accurately model the effect from cyclic loading on clay. One way to model undrained cyclic behavior is to combine, by an Iwan model, several elasto-plastic material models in parallel. This enables the hysteresis effect and the pore pressure build-up to be accounted for. In this thesis the soil behavior is described by the Cam Clay Model, with a degradation term implemented.

1.1 Background

Simulation of cyclic behavior using Iwan models, parallel and series, combined with the NGI-ADP soil model have been done by Grimstad et al. (2014). They concluded that by using an Iwan model combined with several Modified Cam Clay Models(with a degradation term included) a more realistic approach to cyclic modeling would be obtained. This solution would account for the cyclic degradation and it could be used for drained

and undrained cases. The hysteresis effect and the pore pressure build-up(undrained cases) would be simulated. The calculation time was found to be considerable less with the parallel coupling, than series.

1.1.1 Problem formulation

The background of the thesis is to follow up the conclusion made by Grimstad et al. (2014):

Model cyclic behavior of the soil for undrained conditions combining a parallel coupled Iwan model with several Cam Clay Models (degradation included). Will this model be able to simulate the response of clay subjected to cyclic loading?

1.1.2 What remains to be done

Results from the parallel coupling of the Cam Clay Model have to be evaluated. Cyclic triaxial tests are to be preformed which will give a basis for values to expect.

1.1.3 Literature survey

The elasto- plastic theory of soil modeling is primarily based on the knowledge obtained from the course in advanced geotechnical engineering (TBA 4116), as the author completed during the fall semester of 2013. A basis for the theory of cyclic loading is obtained from a textbook from Kramer (2010). An article from Andersen (2009) has been found informative on the practical aspect of modeling cyclic behavior.

1.2 Objective and Scope

To find out if a parallel coupled model is able to simulate the response of clay subjected to cyclic loading, the following objectives are to be accomplished:

- **Theory:** Present the theory that forms the basis in the cyclic model. Relevant theory will primarily be related to Iwan models and the implemented soil model.
- **Modeling:** Make a model that enables parallel coupling of a user-defined soil model and implement this into PLAXIS.
- **Triaxial Tests:** Undrained triaxial tests are to be conducted, cyclic, shear and creep tests.
- **Evaluation:** The results from the cyclic modeling have to be evaluated. Triaxial testing will form a basis in the evaluation of the calculated results. Understanding of the implemented theory will be necessary if any modifications to the model have to be done.

1.3 Limitations

Mass and damping will not accounted for in the cyclic model, which implies a model independent of the frequency of the applied load. The computational capacity defines the limitations regarding size of the problem and the time interval to be modeled, as a general problem when it comes to modeling dynamic behavior of structures.

The yield surface used in the implemented Cam Clay Model don't account for anisotropy. Neither are deformations under constant regarded in this model.

The only type of soil regarded in this thesis is clay. The load response is primarily evaluated under undrained conditions. Increase in pore pressure,

because of no change in original volume, is a typical response related to this type of situation.

1.4 Approach

The model to account for cyclic behavior will be coded in Fortran and designed to work with PLAXIS 2D 2012. The results presented will be calculated by a triaxial test simulation. A triaxial test is easy to simulate in PLAXIS, it is a favorable way to present the hand-calculations from the Cam Clay Model. A triaxial test device was available at the laboratory at NTNU. All results presented is therefore based on the same geometric assumption.

Through the course TBA 4110 Field and Laboratory Investigations the author has obtained detailed information about the soil at a specific site at Stjørdal. Therefore all triaxial tests have been done with samples from this site.

The Cam Clay Model used in this thesis is written by PhD candidate Jon A. Rønningen.

1.5 Outline of Thesis

After a brief introduction to this thesis, theory regarding representation of soil behavior is presented in *Chapter 2*. The elasto-plastic theory forms the basic frame work for the deviation of the equations needed to define the Cam Clay Model. Undrained loading is in focus. A brief summary of the finite element method is presented. This is included to define some of the terms which are frequently used and limitations to this method. *Chapter 3* deals with the soil response from undrained cyclic loading. The Iwan model is also presented in this chapter.

How the pore pressure build-up and the hysteresis effect have been modeled using the FEM program PLAXIS 2D 2012 is explained in *Chapter 4*. The triaxial test procedure and the testing device used in this thesis are presented in *Chapter 5*.

Triaxial results found most relevant are discussed in *Chapter 6*. Some of the results also regards the triaxial device that have been used. *Chapter 7* regards the results from validation and evaluation of the cyclic modeling.

Discussion of the presented results is given in *Chapter 8*. The improvements for further work are also presented. Lastly, *Chapter 9* contains concluding remarks and recommendations for further work on the process of modeling cyclic behavior of clay.

2. Theory

2.1 Elasto- Plasticity

A stress change in a material will cause a response in shape and/ or volume of the structure. In an elasto- plastic theory the total response is divided into an elastic and a plastic contribution. Elastic strains(ϵ^e) are reversible, the original geometry of the structure is restored when the material is brought back to the initial stress state. Plastic strains(ϵ^p) are defined as permanent strains after unloading and they will cause a change in the shape and/or volume of the material. The total strain contribution may be found by adding the elastic and plastic term:

$$\epsilon = \epsilon^e + \epsilon^p \tag{2.1}$$

2.1.1 Elasticity

The relationship between stress and elastic strain is found by introducing a material law, e.g. Hooke's Law. A general form of the elastic strain are defined as:

$$d\boldsymbol{\epsilon}^e = \boldsymbol{D}_e^{-1} d\boldsymbol{\sigma} \tag{2.2}$$

where $\boldsymbol{D_e}$ is the elastic part of the stiffness matrix.

Stiffness
It may be convenient to divided the stiffness into two parts, where one part accounts for change in volume while the other describes change in shape. The stiffness for isotropic elastic materials may be defined by two parameters.

The volumetric stiffness(K), is defined by a change in effective mean stress(p') and volumetric strain(ϵ_{vol}). Using Hooke's Law it may be shown that the volumetric stiffness can be reduced to Nordal (2013):

$$K = \frac{\Delta p'}{\Delta \epsilon_{vol}} = \frac{E}{3(1-2\nu)} \tag{2.3}$$

The elastic shear stiffness may be written as:

$$G = \frac{\Delta \tau}{\Delta \gamma} = \frac{E}{2(1+\nu)} \tag{2.4}$$

2.1.2 Plasticity

When the applied stresses exceeds the elastic capacity the material will get permanent deformations. The plastic strains are often explained by a yield criteria, hardening law and a flow rule. The yield criteria(F) is a limiting surface which, in a stress space, defines an elastic and a plastic area. F<0 implies that the soil is elastic, the material is yielding when F=0 .While the material is yielding the stress change may also cause elastic strains. The hardening law describes change in size and shape of the yield surface as yielding occurs. The development of the plastic strains when the soil is yielding is described with the flow rule. The link between plastic strain and stresses are obtained from:

$$d\boldsymbol{\epsilon}^p = d\lambda \left\{ \frac{\partial Q}{\partial \boldsymbol{\sigma}} \right\} \tag{2.5}$$

where dλ is a plastic multiplier, Q is the plastic potential.

If F=Q the flow rule is associative, otherwise it is non- associative. An associative flow rule implies that the plastic potential($\frac{\partial F}{\partial \sigma}$) always has to be perpendicular to the yield surface. During failure, Eq. (2.5) states that the change in plastic strains will be proportional to the change in the potential, by a factor of dλ.

As the material is yielding, the capacity may change. This is due to a contraction or expansion of the yield surface. Still the criteria that F=0 has to be valid. If the yield criteria is assumed to be a function of the scalar hardening parameter κ, then an infinite small change in the yield surface may be written as:

$$dF = \left\{ \frac{\partial F}{\partial \boldsymbol{\sigma}} \right\}^T d\boldsymbol{\sigma} + \frac{\partial F}{\partial \kappa} d\kappa = 0 \tag{2.6}$$

2.2 Linear Elastic Perfect Plastic Soil Model

The simplest elasto- plastic model is a linear elastic- perfect plastic soil model. All strains below failure are elastic, and plastic at failure. There is no hardening of the soil in this model. When the soil is load to failure, further stress increase is not possible. Unloading will give an elastic response. This is illustrated in Figure 2.1. For simplicity the Mohr Coulomb failure surface for axial compression and the extension, in a p'-q diagram, is assumed equal.

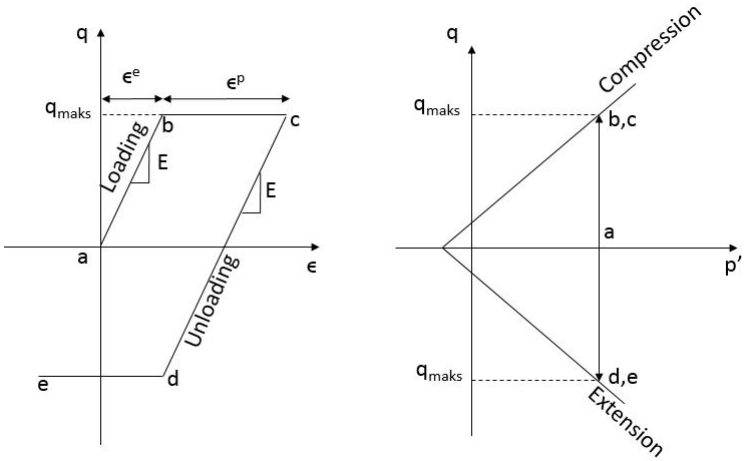

Figure 2.1: Stress path for an elastic perfectly plastic model, after Nordal (2013)

2.3 The Cam Clay Model

The Cam Clay Model(CCM) is an elasto plastic model, which is particularly useful for soft clays where large deformations may occur. If not else specified the derivation of all equations and theory are obtained from Nordal (2013).

The isotropic preconsolidations stress(p'_0) is used as a state parameter. Along with the specific volume(v), the preconsolidation stress is controlling the hardening/softening of the soil structure during yielding . The specific volume is defined as:

$$v = 1 + e \tag{2.7}$$

where e is the void ratio.

The soil response is prescribed in terms of volumetric effective mean stress (p') and deviatoric stress (q). This makes its convenient when comparing to triaxial tests Wood (1990). The strain contribution is therefor divided into an volumetric(ϵ_p) and a deviatoric term(ϵ_q), where each of these terms may further be divided into a plastic and an elastic part.

For triaxial tests the mean stress and deviatoric stress may be simplified and expressed with principles stresses as in respectively Eq. (2.8) and Eq. (2.9).

$$p' = \frac{\sigma'_1 + \sigma'_2 + \sigma'_3}{3} = \frac{\sigma'_1 + 2\sigma'_3}{3} \tag{2.8}$$

$$q = \sigma_1 \ - \sigma_3 \tag{2.9}$$

Elastic Properties

Elastic strains are calculated from the Eq. (2.10).

$$d\boldsymbol{\epsilon}^e = \begin{bmatrix} d\epsilon_p^e \\ d\epsilon_q^e \end{bmatrix} = \begin{bmatrix} \frac{1}{K} & 0 \\ 0 & \frac{1}{3G} \end{bmatrix} \begin{bmatrix} dp' \\ dq \end{bmatrix} \tag{2.10}$$

where the bulk modulus is stress dependent and defined as K=p'v/κ. The shear modulus, G=3K$(1-2\nu)/2(1+1\nu)$.

The shear modulus is assumed constant Wood (1990), resulting that the Poisson's ratio(ν) changes according to the bulk modulus.

Yield Surface and Hardening Function

The yield surface(F) is prescribed as an elliptic yield surface, symmetric about the p'-axis in a p'-q diagram. The symmetry implies that there is no difference in axial compression and extension. The yield surface is defined as:

$$F = q^2 - M^2(p'(p'_0 - p')) = 0 \tag{2.11}$$

M is the inclination of the Coulomb friction angle. For triaxial tests this value may be simplified to Eq. (2.12). The plus or minus sign is valid for respectively triaxial extension and compression tests.

$$M = \frac{6sin(\phi)}{3 \pm sin(\phi)} \tag{2.12}$$

The hardening rule relates how the volume change along with the preconsolidation pressure. These equations are defined as:

$$dv = -\lambda \frac{dp'_0}{p'_0} \tag{2.13}$$

$$dv^p = -d\epsilon_p^p * v = -(-\lambda - \kappa)\frac{dp'_0}{p'_0} \tag{2.14}$$

where λ and κ is the flexibility parameters respectively in the NC and OC area.

Plastic Strain

Plastic strains are calculated from the Eq. (2.15). In the CCM an associated flow rule is used(Q=F). This results that the plastic strains are proportional to the plastic potential. In a p'-q space ϵ_p^p will relate to the horizontal component of$\left\{\frac{\partial F}{\partial \boldsymbol{\sigma}}\right\}$ by a factor of dλ, while ϵ_q^p will change ac-

cordingly to the vertical component.

$$d\boldsymbol{\epsilon}^p = \begin{bmatrix} d\epsilon_p^p \\ d\epsilon_q^p \end{bmatrix} = d\lambda \left\{ \frac{\partial F}{\partial \boldsymbol{\sigma}} \right\} = d\lambda \begin{bmatrix} \frac{dF}{dp'} \\ \frac{dF}{dq} \end{bmatrix} = d\lambda \begin{bmatrix} M^2(2p' - p'_0) \\ 2q \end{bmatrix} \quad (2.15)$$

The expression for dλ is found by setting the values for the plastic volumetric strain(ϵ_p^p) found by the flow rule (Eq.(2.15)) and defined by the hardening rule(Eq.(2.14)) equal to each other. The plastic multiplier, dλ may then be written as:

$$d\lambda = \frac{(\lambda - \kappa)}{vM^2(2p' - p'_0)} \frac{dp'_0}{p'_0} \quad (2.16)$$

The plastic strain(ϵ^p) may then be found be substituting Eq.(2.16) back to the flow rule:

$$d\boldsymbol{\epsilon}^p = d\lambda \left\{ \frac{\partial F}{\partial \boldsymbol{\sigma}} \right\} = \frac{(\lambda - \kappa)}{vM^2(2p' - p'_0)} \frac{dp'_0}{p'_0} \left\{ \frac{\partial F}{\partial \boldsymbol{\sigma}} \right\} \quad (2.17)$$

A FEM program normally applies a strain increment to find the updated stresses. It is therefore of greater interest of finding how the change in stresses (d$\boldsymbol{\sigma}$) and strains(d$\boldsymbol{\epsilon}$) relates to each other. Using the consistency condition from Eq. (2.6), solving for change in the state parameter (κ = p'$_0$), the expression for the change in preconsolidation may be found:

$$dp'_0 = -\frac{1}{\frac{\partial F}{\partial p'_0}} \left\{ \frac{\partial F}{\partial \boldsymbol{\sigma}} \right\}^T d\boldsymbol{\sigma} = \frac{1}{M^2 p'} \left\{ \frac{\partial F}{\partial \boldsymbol{\sigma}} \right\}^T d\boldsymbol{\sigma} \quad (2.18)$$

By using Eq. (2.18), the plastic strain from Eq. (2.17) may be rewritten to

$$d\boldsymbol{\epsilon}^p = \frac{(\lambda - \kappa)}{vM^2(2p' - p'_0)} \left\{ \frac{\partial F}{\partial \boldsymbol{\sigma}} \right\} \left\{ \frac{\partial F}{\partial \boldsymbol{\sigma}} \right\}^T d\boldsymbol{\sigma} \quad (2.19)$$

Total Strain
Adding the elastic strain from Eq. (2.10) and the plastic strain from Eq. (2.19):

$$d\boldsymbol{\epsilon} = \left[\begin{bmatrix} \frac{1}{K} & 0 \\ 0 & \frac{1}{3G} \end{bmatrix} + \frac{1}{A} \left\{ \frac{\partial F}{\partial \boldsymbol{\sigma}} \right\} \left\{ \frac{\partial F}{\partial \boldsymbol{\sigma}} \right\}^T \right] d\boldsymbol{\sigma} \tag{2.20}$$

where A is:

$$A = M^2 p' \frac{v M^2 (2p' - p'_0) p'_0}{(\lambda - \kappa)} \tag{2.21}$$

The expression for the total strain may then be written as:

$$d\boldsymbol{\epsilon} = \left[\begin{bmatrix} \frac{1}{K} & 0 \\ 0 & \frac{1}{3G} \end{bmatrix} + \frac{1}{A} \begin{bmatrix} M^4 (p'_0 - 2p')^2 & -M^2 2q(p'_0 - 2p') \\ -M^2 2q(p'_0 - 2p') & 4q^2 \end{bmatrix} \right] d\boldsymbol{\sigma} \tag{2.22}$$

The stress increment may then be found by:

$$d\boldsymbol{\sigma} = \boldsymbol{D}_{ep} d\boldsymbol{\epsilon} \tag{2.23}$$

where $\boldsymbol{D}_{ep}$ is the total stiffness matrix.

The expression for the total stiffness matrix is found in relevant literature.

2.3.1 Undrained loading

The criterion of no volumetric change during undrained conditions will affect the development of strain and stresses. This criterion directly applies to the volumetric strains(ϵ_p). The equations from the hardening law still has to hold, and by this induce a change in the deviatoric stresses(ϵ_q).

Elastic Loading
Elastic loading will result in no change in the mean effective stress, as shown in Eq. (2.24). The effective stress path in a p'-q plot is therefor a straight vertical line.

$$dv = dv^e = -d\epsilon_p^e * v = \frac{dp'}{K} = 0 \Rightarrow dp' = 0 \tag{2.24}$$

This implies that there can be no change in deviatoric strain as well ($d\epsilon_q^e = 0$).

Plastic Loading

As the material is yielding and the plastic strains develop, the total change in specific volume may be written as:

$$dv = dv^e + dv^p = 0 \tag{2.25}$$

The change in specific volume(dp_0') may then be found by combining the equations from the hardening rule. Expressed by infinitesimal stress increments:

$$dv = dv^e + dv^p = -\kappa \frac{dp'}{p'} - (\lambda - \kappa)\frac{dp_0'}{p_0'} = 0 \tag{2.26}$$

In terms of the stress increment(dp') the new preconsolidation stress may be calculated. The change in deviatoric stress is found by inserting $q = q_0 + dq$ and $p' = p_0' + dp'$ into the flow rule (Eq.2.11).

When the change in preconsolidation(dp_0') stress and deviatoric stress(dq) are know dϵ_q may be calculated:

$$d\epsilon_q = d\epsilon_q^e + d\epsilon_q^p = d\epsilon_q^e + d\lambda(\frac{dF}{dq}) = \frac{1}{3G}dq + \frac{2q(\lambda - \kappa)}{M^2\nu(2p' - p_0')}\frac{dp_0'}{p_0'} \tag{2.27}$$

CSL:
Regardless of the initial condition the soil will end up at the Critical State Line(CSL). The numerator in Eq. (2.27) will go towards zero, as the effective stress approaches p'$_0$/2, which lead to $d\epsilon_q \to \infty$. The yield surface will stop moving and we have reached the Critical State. No further change in deviatoric stress may occur. The stress path for a normally consolidated(NC) and an overconsolidated sample(OC) is presented in Figure 2.2.

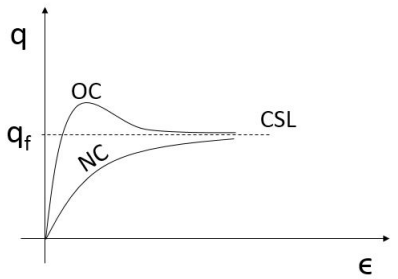

Figure 2.2: Critical State

Stress Path
Two stress states are presented to explain how the stresses will develop towards failure. One test is a highly overconsolidated (OC) test, while the other is slightly consolidated sample (NC).

For the NC case the plastic strains would make the sample dilate. This is illustrated in Figure 2.3a, showing the change in plastic potential. The elastic strains has to force the sample to contract, zero volumetric change. The sample will move towards the critical state line. This will cause an expansion of the yield surface, the soil is hardening.

As for the OC case, Figure 2.3b, its the opposite case. The yield surface will contract, and cause softening.

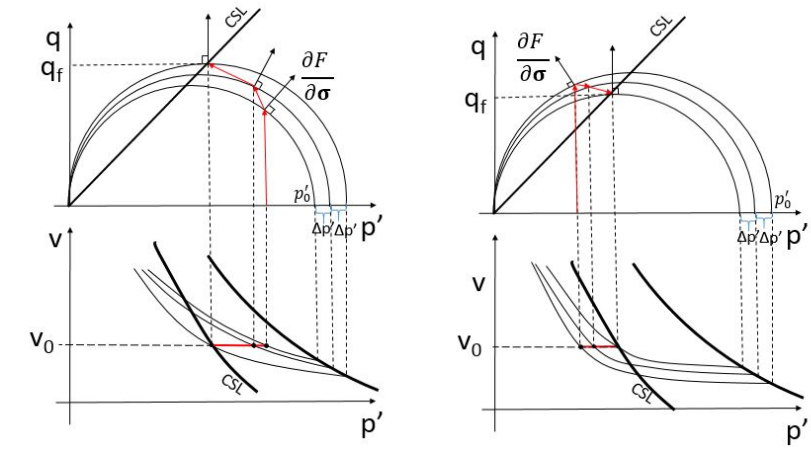

(a) Slightly OC, Wood (1990) (b) Highly OC, Wood (1990)

Figure 2.3: Stress path undrained loading Cam Clay

2.3.2 Softening

Degradation or softening of the structure implies that the plastic strains are increasing for a decreasing yield stress or contracting yield surface Nordal (2012). This will results that the residual deviatoric stress is lower than the peak stress.

Undrained loading of overconsolidated samples in the Cam Clay Model will results in a lower residual strength than the peak strength, illustrated in Figure 2.2. A softening of the structure will occur as the yield surface is contracting.

If degradation of the structure is explicitly included into the soil model the yield surface may contract further and the capacity of the soil will be reduced illustrated in Figure 2.4. The softening will then apply to both the overconsolidated and normally consolidated case.

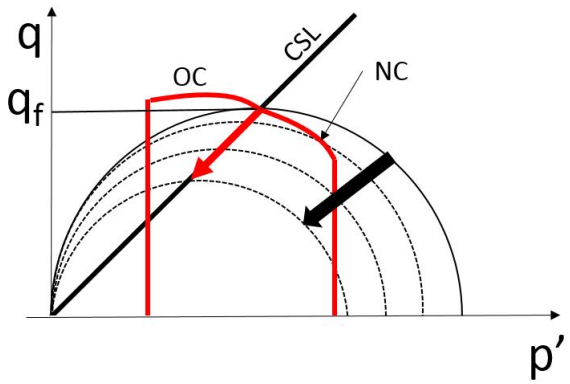

Figure 2.4: Softening in the Cam Clay model

2.4 Finite Element Method

The Finite Element Method (FEM) is a mathematical model for solving boundary value problems. The structure is discretized (meshed) into small pieces (elements), then properties and functions at all elements are evaluated. Together all elements describe the total behavior of the structure.

Discretization of the domain makes the FEM an approximate method, but the results is often within acceptable tolerance limits. The more elements generated inside a domain, the less the error but increased cost of calculation.

The shape of the elements may vary, and they are often chosen based on a compromise between accuracy and calculation time Hughes (2000). The FEM program PLAXIS automatically discretize the domain into triangular elements, where the user may choose between 6 or 15 node elements Plaxis (2012b). The user may also choose the coarseness of the discretization, number of elements inside the domain.

Integration of mathematical functions has to be evaluated over the element

domain for representation of the element behavior, e.g. stiffness matrix. Instead of numerically evaluate these functions over the element domain, it may be used some methods to save calculation cost. PLAXIS is using a method called Gaussian Quadrature Plaxis (2012c). Instead of integrating the mathematical function over the whole domain, the functions are evaluated at certain points which lies inside the element domain or at the boundary. Each point are weighted according to its position, the position will depend on the shape of the element and number of integration point. These points are referred to as Gauss points. The 6 node element in PLAXIS consists of 3 Gauss points, while the 15 node element has 12.

The finite element method may give inaccurate results in problems where large deformations occurs. As the displacements become so large that they alter the distribution or orientation of the applied load or the orientation of the internal forces and moments numerical inaccuracy and instability problems may arise Cook et al. (2002). Some of the problem lies in that the formulation of the elements is not refereed to where they are, but where they was originally. Updated mesh may be used to solve this problem but it is a time consuming process and numerical errors may still occur when the information is transfered from previous to the update Gauss point Cook et al. (2002).

3. Cyclic Loading

Cyclic loading may cause change in the stiffness and strength of the soil. Some of the most important factors that influence the effect of cyclic loading are: cyclic strain, strain amplitude, void ratio, mean principal effective stress, plasticity index, overconsolidation ratio and number of loading cycles Kramer (2010).

Expected frequencies at given situations are presented in Table 3.1.

Table 3.1: Frequencies at given situations Head (1986)

Situation	**Frequency of load application**
Offshore structures	Tidal effects: usually 2 cycles pr day Wave effects: several cycles pr minute
Wind loading	0,01 - 0,1 Hz
Earthquake on structures	0,1 -10 Hz
Sub-base for road, railways	10 - 100 Hz
Foundation for machinery	Up to 100 Hz

3.1 Stresses and Strains

The total shear stress (τ_{tot}) may be divided into two parts, average (τ_{ave}) and cyclic (τ_{cyc}) shear stress. These will vary with time as the frequency, amplitude and load changes. If the monotonic shear stress is assumed constant with time, the total shear contribution may be written as:

$$\tau_{tot}(t) = \tau_{ave} + \tau_{cyc}(t) \tag{3.1}$$

The total shear strain is divided into two parts, cyclic (γ_{cyc}) and permanent strain (γ_{ave}.) The cyclic strain are reversible and may increase with time, illustrated in Figure 3.1a. Permanent strains are obtained when the cyclic load causes different start and ending position for a cyclic loop.

Both γ_{cyc} and γ_{ave} will depend on τ_{ave} and τ_{cyc} when the stresses are larger than zero. It has been shown for marine clays that γ_{cyc} depends mainly on τ_{cyc} and likewise relationship between γ_{ave} and τ_{ave} has been found Kramer (2010).

The shear stiffness is related to the inclination of the cyclic loop. As shown in Figure 3.1b the inclination of the loop varies, meaning that the shear stiffness is not constant through the cyclic loop. The G_{tan} value describes how the shear stiffness varies with time. The steepest inclination of the loop indicates the largest value of the shear modulus, G_{max}. G_{sec} indicates the average shear stiffness for a single loop.

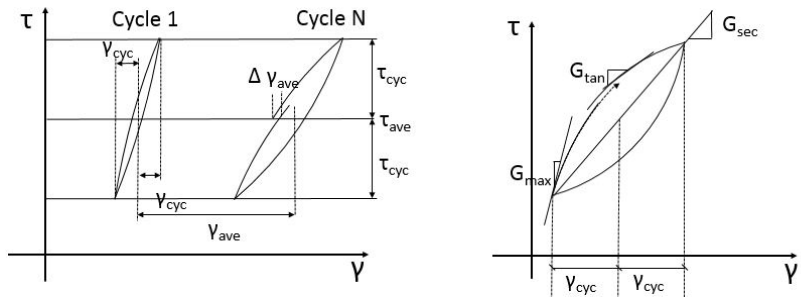

(a) Cyclic and average (b) Shear stiffness

Figure 3.1: Shear strain during cyclic loading Andersen (2009)

The stiffness of the soil changes through a cyclic load period, among other factor cyclic amplitude and duration of the load will affects this. The inclination of the secant value through a cyclic test will tell us if the soil is stiffening or loosening.

As for the strain and stresses, the pore pressure may also be divided into

an average (u_0) and a cyclic part(u_{cyc}), Eq. (3.2). The cyclic part of the pore pressure will change according to the applied load and degradation of the structure Andersen (2009).

$$u = u_0 + u_{cyc} \tag{3.2}$$

3.2 Properties of Soil

Engineering problems, foundation work, slop stability etc., for the type of situations presented in Table 3.1 is affected by the strength the soil can mobilize at high strains. Two important aspects of cyclic loading is the degradation of the soil structure and hysteresis effect. For undrained loading the degradation governs the pore pressure build-up, and therefore influence the capacity. The hysteresis effect will be a damping factor in the system.

3.2.1 Degradation

Cyclic loading has a tendency to break down the soil structure and reduce the capacity of the soil. The maximal shear strength during cyclic loading ($\tau_{cyc,f}$) is therefor, in general lower than the maximal monotonic shear strength(τ_f), illustrated in Figure 3.2.

The soil grains may form a denser state when they are subjected to repeated loading. During undrained conditions there can be no volume change, because water is approximately incompressible. The soil grains will therefore occupy less portion of the volume. This causes the pore pressure to increase as more and more of the cyclic load is transfered directly to the pore water. An increase in pore pressure will cause a reduced effective stresses and may further result in permanent strains.

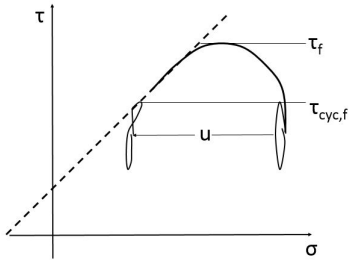

Figure 3.2: Cyclic and monotonic shear stress after Andersen (2009)

3.2.2 Hysteresis effect and damping ratio

A hysteresis effect is present when no strains has accumulated in a sample which are loaded and then unloaded, but more energy is used to load the sample than is returned from unloading it.

Based on elastic theory, there should be no dissipation of energy at small strain. Experiments has showed that some energy is dissipated even at small strains Kramer (2010). The form of the hysteresis loop is linked to the damping ratio. An increasing cyclic loop will represent a larger damping in the soil. The damping ratio is also linked to the cyclic amplitude, and will increase with increasing cyclic amplitude Kramer (2010). The damping ratio may be calculated from Eq.(3.3).

$$\xi = \frac{1}{2\pi} \frac{A_{loop}}{G_{sec}\gamma_{cyc}^2} \tag{3.3}$$

3.3 Modeling the Hysteresis Effect

Modeling cyclic behavior of soils may be done in different ways. One possibility is to recreate the hysteresis effect in the soil by an Iwan model Houlsby and Puzrin (2006), in combination with an elasto-plastic soil model Grimstad et al. (2014).

An Iwan model consist of groups of spring and slider. By assigning an elasto-plastic soil model with different set of material parameters to each of these groups, the strain- stress curve shown in Figure 3.1b can be calculated. This will account for a more realistic modeling of cyclic behavior.

3.3.1 Iwan models

A great advantage of using a Iwan model is that no additional parameters are needed, the parameters used is only linked to the soil model included. Coupling of structural elements, with Iwan models, may be done in two different ways, parallel or series.

The stiffness at each spring is calculated by the soil model and the material properties assigned to that group. The slider will adjust for when the maximum capacity is reached (parallel) or for which stress level plastic deformations occurs(series).

Each of these groups in the Iwan model will have different capacity, stiffness, plastic limit, etc. according to the material parameters assigned. This enables that for a given stress state, the total response may be combination between elastic and plastic deformation.

Series:
In series coupling all elements are applied the same amount of stress, illustrated in Figure 3.3.

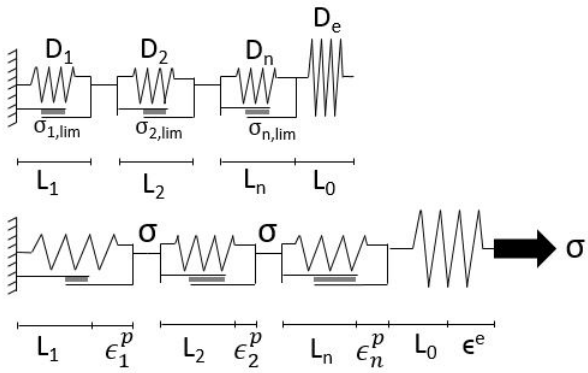

Figure 3.3: Series coupling of an Iwan model, after Houlsby and Puzrin (2006)

Any change from the initial length(L_i) will cause strains to the spring. The original series coupling model from Iwan consist of one elastic spring and a series of element with a individual slip stress Houlsby and Puzrin (2006). The slip stress for each spring is represented by $\sigma_{i,lim}$, stresses over this value will result in plastic strain. The slider is not initialized before the stress in the spring exceed the slip stress.

The elastic response is described as the elongation of the elastic spring, while elongation on the other give plastic strains. The total strain may be found from Eq.(3.4).

$$\epsilon = \epsilon^e + \sum_{i=1}^{n} \epsilon_i^p \tag{3.4}$$

The total stiffness is calculated from Eq. (3.5),

$$\frac{1}{D_n} = \frac{1}{D_e} + \sum_{i=1}^{n} \frac{1}{D_i} \tag{3.5}$$

The total elastic stiffness(D_e) will be a summation of the elastic stiffness for each individual spring.

The in inverse ratio in the calculations of the stiffness explains how the stiffness decrease as more and more spring are activated.

For each time a stress is applied, finding the respective strain in each spring will be an iterative process. This will be a function depending on the stiffness and plastic limit of each spring. This make series coupling a more time-consuming iteration process than parallel coupling Grimstad et al. (2014).

Parallel:
Parallel coupling leads to that all the elements will get the same deformation, as illustrated in Figure 3.4.

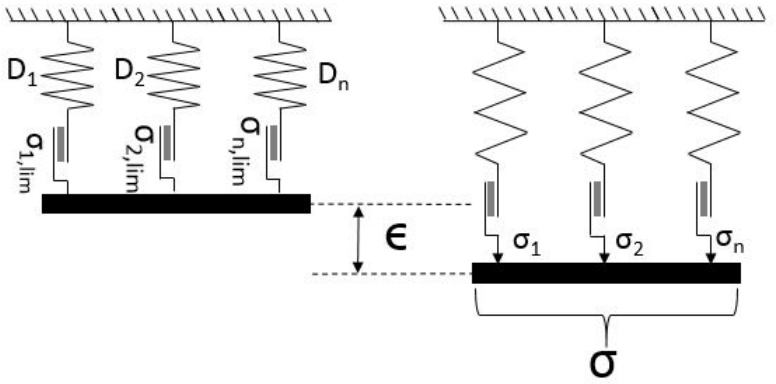

Figure 3.4: Parallel coupling of an Iwan model

The stiffer the spring, relative to the others, the larger part of the total stress it will attract. The slider is supposed to illustrate that when the stress in the spring exceeds the failure load the spring will become inactive ($\sigma_i > \sigma_{i,lim}$), resulting that stiffness will be zero. The capacity at each spring will depend on the soil model and material parameters used in that particularly spring.

The total stress (σ) is found by adding the stresses at each spring(σ_i):

$$\sigma = \sum_{i=1}^{n} \sigma_i \tag{3.6}$$

Similarly the total stiffness (D) is found:

$$D = \sum_{i=1}^{n} D_i \tag{3.7}$$

4. Modeling Cyclic Soil Behavior using FEM

Modeling cyclic soil behavior has been done by combining a parallel coupled Iwan model with several elasto-plastic soil models. The hysteresis effect is accounted for by assigning different material properties to each elasto-plastic model. Degradation of the soil structure is included into the soil model to reflect the pore pressure build-up during undrained cyclic loading. A user-defined model has been implemented into the finite element program PLAXIS 2D 2012 to calculate the effect.

4.1 User-Defined Soil Models in PLAXIS

In PLAXIS it is possible to add user-defined (UD) soil models. This option allows new and modified material models to be implemented into the program. PLAXIS provides time and stress increments and the implemented model is used to calculate updated stress and state variables Plaxis (2012a).

Implementation of an Iwan model into PLAXIS is done by a user-defined script. This user-defined script enables several set of material parameters at each Gauss point. This script is further referred to as the Multi Parameter Script (MPS). A user-defined soil model has to be included into the MPS to represent the soil behavior. Since the response of clay is of interest, a Cam Clay Model with degradation of the structure is chosen.

All UD soil models must follow a fixed subroutine setup. A description of this process is found in Plaxis (2012a).

4.1.1 Iwan model in PLAXIS

The calculation process for a parallel coupled Iwan model, combined with a user-defined soil model, is illustrated by a simplified flow chart in Figure 4.1. A soil model, consisting of m state variables, coupled by n number of groups is used to demonstrate the process. Each group is representing a spring and a slider in the Iwan model. The operations in the red boxes, Figure 4.1, is repeated n-times.

The calculation process starts with initialization of stresses and state variables at each group. The initial stress(Sig0) is divided among the groups in the Iwan model. Distribution of the initial stresses are described in Section 4.1.2. With stresses and state variables known a strain increment(dEps) is applied. The same strain increment is applied to all groups in the Iwan model. Along with the strain increment, the previous stresses(Sig0i) and state variables(StVar0i) at each individual group are used to calculate updated stiffness matrix(Di), stresses(Sigi) and state variable(Stvari).

The total stiffness matrix (D), stress (Sig) along with the state variables (StVar) are summed and returned to PLAXIS. These values, with a new strain increment, are then used as the input parameters at its respective group in the new calculation step.

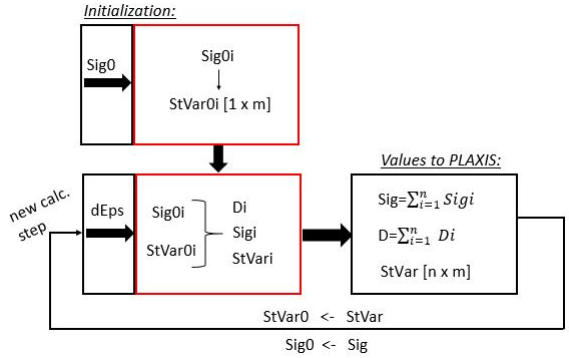

Figure 4.1: Flow chart of parallel coupling in PLAXIS

A user manual for the MPS is added in Appendix E and the Fortran program code is added in Appendix F.

4.1.2 Distribution of initial stresses

Stresses are distributed, among the included groups in the Iwan model, based on the assumption of that all groups are assigned with the same volumetric stress(p') and an equal preconsolidation(p'_0). The initial stress values at each element is calculated based on expression of the preconsolidation, presented in Eq. (4.1).

$$\begin{aligned} F &= q^2 - M^2(p'(p'_0 - p')) = 0 \\ p'_0 &= \frac{q^2}{M^2 p'} + p' \end{aligned} \tag{4.1}$$

A Fortran code of the implementation of the stress distribution for a triaxial test simulation is added in Appendix F.

Isotropic stress state:
An initial isotropic stress condition($q = 0$) Eq. (4.1) is reduced to:

$$p'_0 = p' \tag{4.2}$$

Eq. (4.2) still has to hold as the stresses are distributed among n number of elements:

$$p'_{0,1} = p'_1 = p'_{0,2} = p'_2 = ... = p'_{0,n} = p'_n \tag{4.3}$$

This implies that for an isotropic stress state the initial stresses has to be divided equally to all groups in the Iwan model.

Anisotropic stress state:
For Eq. (4.1) to hold in an anisotropic stress state($q > 0$), the deviatoric stress has to differ depending on the M value assigned to each model. Since

p' and p'_0 are assumed equal in all n number of elements, Eq. (4.1) may be reduced to:

$$p'_{0,1} = p'_{0,2} = ... = p'_{0,n} \tag{4.4}$$

$$\frac{q_1^2}{M_1^2} = \frac{q_2^2}{M_2^2} = ... = \frac{q_n^2}{M_n^2} \tag{4.5}$$

The deviatoric stress is per definition positive. A general expression may be stated, Eq. (4.6), combining the relationship between deviatoric stress(q_i) at each element and the assigned strength(M_i).

$$\frac{q_i}{M_i} = const. \tag{4.6}$$

Even though the stresses are unequally distributed the deviatoric stress at each element has to be summed up to the total deviatoric stress:

$$\sum_{i=1}^{n} q_i = q \tag{4.7}$$

Combining Eq. (4.6) with Eq. (4.7) the relationship between deviatoric stress and strength may be found:

$$const. = \frac{q}{\sum\limits_{i=1}^{n} M_i} \tag{4.8}$$

For a triaxial test the following identities has to hold:

- $p' = \frac{1}{3}(\sigma'_x + \sigma'_y + \sigma'_z)$
- $\sigma'_x = \sigma'_z$
- $q = \sigma'_y - \sigma'_x$

Based on these identities, along with the deviatoric stresses from Eq. (4.6) and the known p' value at each element, the principal stresses at each group may be found.

4.1.3 Representation of the soil

The behavior of the soil is represented by a user-defined Cam Clay Model(CCMD), which accounts for degradation of the soil structure. Input parameters need for this user-defined model are given in Table 4.1.

Table 4.1: Input parameters for the user-defined Cam Clay Model

$\boldsymbol{\kappa}$	$\boldsymbol{\lambda}$	**G**	$\boldsymbol{e_0}$	**M**	**OCR**	$\boldsymbol{x_0}$	$\boldsymbol{a_p}$	$\boldsymbol{a_q}$
(-)	(-)	(kPa)	(-)	(-)	(-)	(-)	(-)	(-)

where the constants x_0, a_p and a_q controls the degradation.

None of the user-defined constants controlling the degradation reflects a specific material property. They rather has to evaluated as a numerical solution of the degradation in the soil. The preconsolidation found by the initial stress state(Eq. (4.1)) multiplied by the OCR defines the initial preconsolidation in this model.

Degradation:
Degradation is accounted for by reducing the preconsolidation when the soil is yielding, which implies a change to the yield surface. Development of plastic strains are dependent of the yield surface(Q=F), which causes the stress path to be dependent of the degradation term.

The initial value of the preconsolidation is unaffected by the degradation term. When the degradation term is included a factor of $(1 + x_0)$ is added into the expression of the preconsolidation. A reduction in x_0 will then cause a reduced preconsolidation. The input value from Table 4.1 is used as an initial value of x_0. The change in x_0 is defined as:

$$\frac{dx_0}{d\lambda} = x_0\left(a_p\left|\frac{\partial Q}{\partial p'}\right| + a_q\sqrt{\frac{2}{3}\left\{\frac{\partial Q}{\partial \boldsymbol{\sigma_d}}\right\}^T\left\{\frac{\partial Q}{\partial \boldsymbol{\sigma_d}}\right\}}\ \right) \tag{4.9}$$

by setting $x_0 = 0$ clearly no degradation should occur.

The degradation term will stabilize at a value determined by the combination of the terms in Eq. (4.9). Increasing the constants controlling the degradation a greater reduction in both p' and q will follow. Figure 4.2 illustrates the effect of the user-defined constants controlling the degradation.

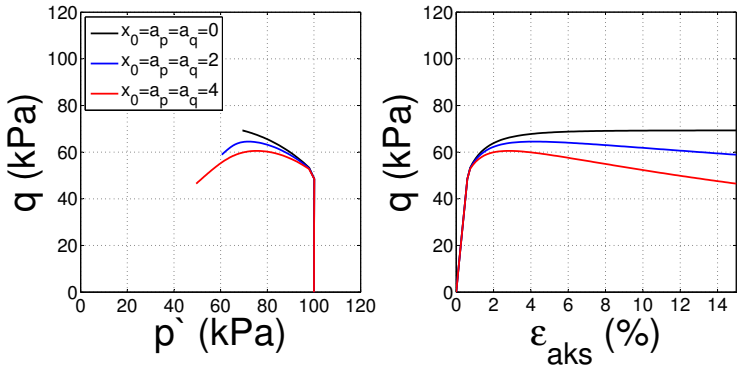

Figure 4.2: Effect of the degradation constants in the UD Cam Clay model

A change in a_q is highly more effective than a change in a_p. A ratio of $a_p/a_q \approx 1/3$ is recommended for practical use.

4.2 Modeling Soil Response from Cyclic Loading

Hysteresis effect and the pore pressure build-up is accounted for in the modeling of soil behavior during cyclic loading. By the degradation term, in the implemented soil model, the average pore pressure is calculated. A linear elastic perfect plastic soil model are used in the Iwan model to illustrated how the hysteresis effect has been modeled. The same principle is still valid for more advanced soil models.

4.2.1 Pore pressure build-up

The stress path for a slightly overconsolidated sample, repeatedly loaded and with a degradation term included is illustrated in Figure 4.3. If there had been no degradation present, the preconsolidation would not have changed after the sample had reach the CSL. Further cyclic loading would have resulted in an elastic behavior. The degradation term will force the yield surface to contract until a stabilized value, determined by Eq. (4.9), has been reached. Increased pore pressure will be a result from that the effective stresses are reduced.

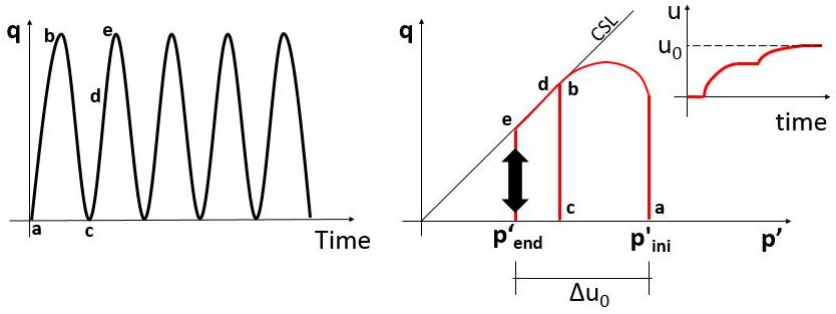

Figure 4.3: Undrained cyclic loading of a soil model with degradation included

Using an Iwan model to couple several of the CCMD will result in a mixed behavior depending on the material properties assigned to each element. The amount of degradation pr cycle in each element will depend on the strength of the other elements in the model. Each model will contribute to an increase in the average pore pressure according to the degradation in that model.

4.2.2 Hysteresis effect

Including an elasto plastic soil model into the Iwan model, the hysteresis effect may be modeled. A linear elastic perfect plastic soil model is used to illustrate how the hysteresis effect has been modeled.

If only one spring is included the response will be a straight line back and forth, as long as the applied load does not exceed the yield strength (σ_{lim}). When the applied stress are equal to the yield strength a response equal to Figure 2.1 will be simulated. As more springs are included, with different set of material properties, the total response will look more and more like a rounded hysteresis loop.

At the start all spring will have an elastic behavior. When the loading exceeds a certain limit($\sigma_{1,lim}$) the first spring will start yielding and the stiffness for that spring is zero. This reduces the total stiffness of the system. As more and more springs starts yielding the total stiffness is further reduced.

When unloaded, all spring kicks in immediately. When the spring reaches its maximum capacity the slider account for the plastic deformations. That's why the stiffest behavior during unloading is observed at the start. The first yield point while unloading will be when the difference between the maximum capacity and the stress unload has reached a value of ($2\sigma_{1,lim}$)

The change in stiffness according to the applied cyclic load is illustrated in Figure 4.4.

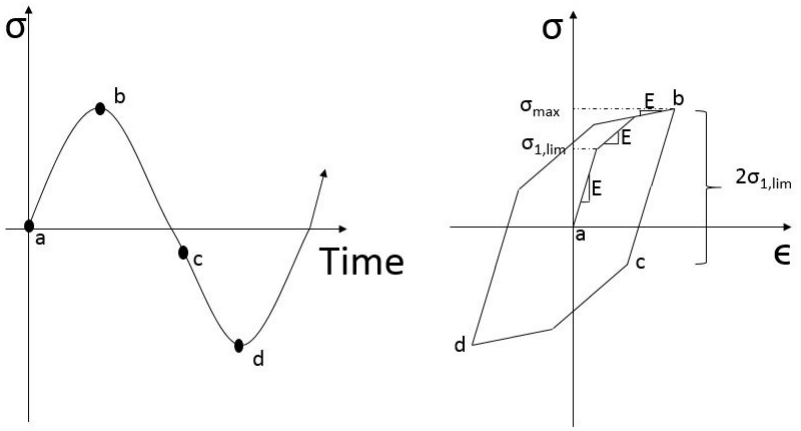

Figure 4.4: Cyclic stress path and stiffness, after Houlsby and Puzrin (2006)

If there is no change in the applied load, change in stiffness or accumulation of strain the calculated cyclic loop will only follow the same path.

5. Triaxial Test

In geotechnical design stiffness and strength parameters of the soil are essential to preform any numerical analysis. Theses parameters and the behavior of the soil may be found and evaluated from a triaxial test preformed on representative soil sample.

5.1 Test Procedure

The triaxial test procedure may be divided into three separate phases

- Installation
- Consolidation
- Loading/ failure

5.1.1 Installation

The sample is mounted inside the triaxial cell, and the cell is filled with water. The sample has an initial area(A_0) of 5,4 cm^2 and height(h_0) of 10 cm.

5.1.2 Consolidation

The sample is brought to a desirable stress state under drained conditions. This is done by an increasing water pressure causes an equally distributed pressure on the sample. An additional vertical load is applied if the consolidation is anisotropic. During the consolidation the amount of water

squeezed out of the sample is measured and the updated area is calculated. An effective stress state equal to the in situ stress state defines a K_0' consolidation.

5.1.3 Loading/ failure

The loading/failure of the soil sample can by done by shear, cyclic or creep, or by a combination between any of these phases. All phases may be done drained or undrained.

- **Shear:** A constant rate of strain is applied. The strain rate depends on the sample tested. 1,5 %/h is normally used for fat clays Sandven et al. (2013).

- **Cyclic:** A strain or stress amplitude is applied, additional static load may also be added. The frequency of the cyclic load amplitude(τ_{cyc}) or cyclic strain amplitude(ϵ_{cyc}) has to be set.

- **Creep:** A constant load is applied for a period of time.

5.1.4 Sample disturbance

During consolidation the volume change is equal to the amount of water drained from the sample. The amount of water drained may indicate the sample quality. Using the volumetric strain as a basis, $\epsilon_{vol} = \Delta V/V_0$, the sample quality may be estimated based on the values in Table 5.1

Table 5.1: Sample quality based on expelled water Sandven et al. (2013)

OCR	**Depth**	**Perfect**	**Acceptable**	**Disturbed**
		$\epsilon_{vol}<$	$<\epsilon_{vol}<$	$\epsilon_{vol}>$
(-)	(m)	(%)	(%)	(%)
1,0-1,2	0-10	3,0	3,0-5,0	5,0
1,2-1,5	0-10	2,0	2,0-4,0	4,0
1,5-2,0	0-10	1,5	1,5-3,5	3,5
2,0-3,0	0-10	1,0	1,0-3,0	3,0
3,0-8,0	0-10	0,5	0,5-1,0	1,0

The samples tested in thesis are from 80 cm long cylinders, with a diameter of 54 mm. The sample quality from 54 mm cylinders normally decreases towards the end pieces. Perfect quality samples are rarely obtained with this cylinder size Sandven et al. (2013).

5.1.5 Back pressure

The use of back pressure in the triaxial cell may reduced the effect of air bubbles in the system Head (1986). Air inside the system will be a damping factor and at higher pressure the air bobbles will get a stiffer behavior. Higher pressure will also cause the air bobbles to more easily be dissolved in the water Head (1986) .

5.2 Test Device Used

A simplified model of the triaxial testing device used in this thesis is shown in Figure 5.1

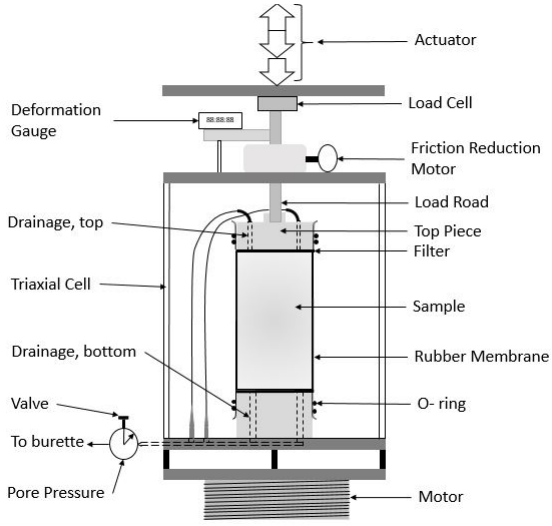

Figure 5.1: Triaxial test device used

This device enable cyclic tests which are stress or strain controlled. A strain rate is applied with the motor at the bottom, and the actuator at the top applies force. It is not possible to use the motor and the actuator at the same time. If the motor is activated the actuator has to be rigid and the other way around. The motor step may be used to measure deformation.

The load rod is pressed up against the load cell. The connection between the load rod and the load cell is based only on compression. The applied vertical load always has to be greater than the horizontal load. This leads to that negative shear stresses may not be applied.

To reduce friction between the load rod and triaxial cell oil is added at the top part inside the triaxial cell. There is also mounted a friction reduction

motor.

A valve is controlling if the test is drained or undrained. For drained conditions the water may drain from both top and bottom. The water drains into a closed burette where the amount of water is measured. When the valve is closed no water may drain from the sample, and the change in pore pressure is measured.

When placing the deformation gauge to the load rod it is necessary to mount the gauge as far up on the rod as possible. As the sample deform the gauge will move down towards the top of the triaxial cell. When the sample has reached sufficient deformation the gauge will come in contact with the top of the triaxial cell and further deformations of the sample is not registered by the deformation gauge. This may also cause some disturbance to the soil sample. The deformation gauge used is only able to measure displacements up to 13,5 mm. If it is desirable to measure values greater than this, the gauge has to be moved further up on the load rod during the test. Care should be taken if this has to be done, this may easily cause disturbance to the soil sample.

The software controlling the triaxial test does not correct for a change in the sample area during the cyclic test. This causes the stresses to decrease as the sample area increases. The reason that this is not included is that this would have disabled the possibility for adjusting and resetting the deformation gauge during a test.

The cell pressure and the static load applied with the actuator has to be set manually. The compression force between the load rod and the load cell measures the applied force. Cell pressure and static load has its own valve that has to be set to the desirable value. The response from the adjustment of the valves may be seen at the computer right away. It may take a small amount of time to adjust the valves so the correct load is applied, because the system has to stabilize.

6. Results from Triaxial Tests

In total there have been done seven triaxial tests. Information and results from all tests are presented in Appendix B. All tests are conducted on Stjørdal clay in the depth interval 10,6-11,6 m. Detailed information at the site and the soil are obtained from Frydenberg et al. (2013). The frequency at all cyclic phases was set to 0,1 Hz.

The presented results also deals with observations related to the triaxial device used. Leakage related to use of back pressure resulted that none of the tests were conducted with back pressure.

6.1 Measured Pore Pressure

The pore pressured is measured at the top and bottom of the soil sample and it is assumed to be representative for the stress situation throughout the entire sample. However due to low permeability in the soil, the pore pressure build-up inside the sample is not registered right away. For a small amount of time, it is observed only a slightly change in the pore pressure. The difference between change in effective and total stress will mainly depend on the average pore pressure measured. The shape of the curves in the triaxial results presented may be mistaken for the total stress path, which then not are the case.

The cyclic change in pore pressure is barely registered in the triaxial testing device. The cyclic tests where this term is observed are presented in Appendix C. A general trend in these results are a slight increase in the cyclic pore pressure towards the end of the cyclic phase.

6.2 Friction

Friction in the system is the result from contact between the load rod and the triaxial cell. Areas where friction occurs in the system are circled in Figure 6.1

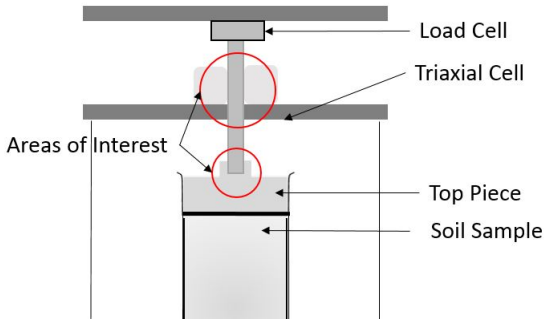

Figure 6.1: Areas where friction occurs

6.2.1 Interaction load rod and triaxial cell

To estimate the friction a rubber sample, with equal shape as a soil sample, was mounted inside the triaxial cell. The cell pressure was set to roughly 80 kPa and 40 kPa in additional vertical load was added.

The friction is estimated under two strain amplitudes(ϵ_{cyc}). The highest amplitude was set to ± 100 μm, Figure 6.2a, and the lowest was set to ± 10 μm, Figure 6.2b. In both of the figures, "On" implies that the friction reduction motor is activated. Hysteresis in the rubber sample is checked and was found to be neglected. The strain has been measured with the deformation gauge. Oil was added at the top of the triaxial cell to reduce friction.

There was expected that no energy to dissipate from this test, this would have resulted in straight lines back and forth.

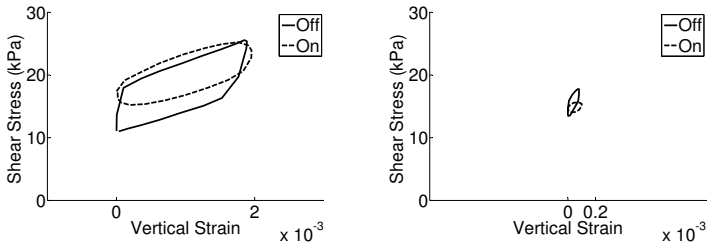

(a) $\epsilon_{cyc} = \pm 100\mu$m (b) $\epsilon_{cyc} = \pm 10\mu$m

Figure 6.2: Cyclic loading of a rubber sample

A closer lock up at the interaction between the load rod and the triaxial cell was made. This inspection concluded that if the load rod is not placed completely centric high friction forces will easily occur. The testing was done by pressing the load rod in contact with the cell and estimate the friction force by hand.

6.2.2 Further evaluation

Influence of friction in the system is further evaluated by inspecting the results from two of the tests conducted. The test from 11,2m, Figure 6.3a, is load controlled and deformation is measured with the deformation gauge. A strain amplitude was applied the test from 11,6m, Figure 6.3b, and the motor is used to measure deformations.

The sample for 11,6m shows almost no dissipation of energy for the first cycle. The small energy loss at the bottom of the cycle is probably related to the gear ratio in the motor. It is not known for the later cycles how much of the energy loss that is due to hysteresis effect in the sample and friction force in the system.

By the shape of the load controlled cycles in Figure 6.3a, friction is presented and is highly affecting the results.

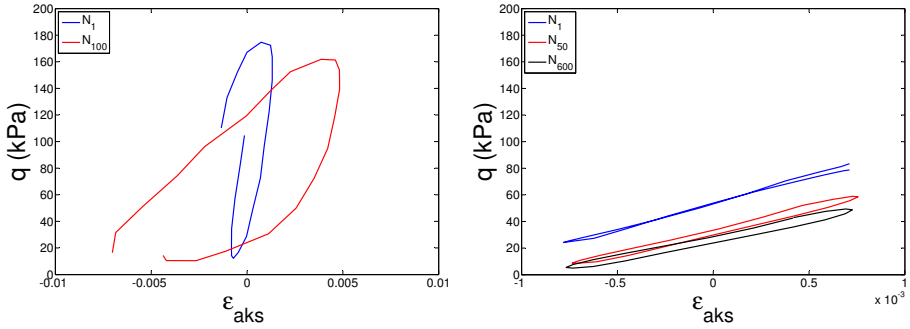

(a) Depth: 11,2m. Load controlled (b) Depth: 11,6m. Strain controlled

Figure 6.3: Friction from two cyclic triaxial tests

It has been found no connection between how the force is applied the sample(motor or actuator) and the friction in the system. The low friction observed in the strain controlled test, is likely to come from that this sample was better build into the triaxial cell.

6.2.3 Conclusion

Results from the triaxial tests are easily affected by the friction between the load rod and triaxial cell. The friction seems to vary through a cycle, resulting in loops with an uneven contour. Results shows that the friction reduction motor is more effective at low strains, because the friction force is increasing according to the cyclic amplitude. For tests that endured for a long period of time it was observed that the oil added during the installation process was pressed out of the triaxial cell.

The user have little control of how the friction in the system will develop after the cyclic triaxial test has started. Before the test is started the load rod is inserted into the top piece. At the start of the test, the interaction between the load rod and triaxial cell, is largely controlled by how the sample is build into the cell. As the sample starts to deform movement

and rotation of the top piece may easily occur. This will cause horizontal force or moments to be transfered to the load rod which results in friction forces. It is be complicated to separate the energy loss due to friction and the hysteresis in the soil, since the friction is a function of more than just the cyclic amplitude. It will also vary from test to test.

Friction between the triaxial cell and the load rod will inflict differently on the measured load, depending if strain is applied with the motor or force is applied with the actuator. When the motor is in use, the friction will cause a deviation between the measured values by deformation gauge mounted to the load rod and the applied deformation with the motor. When a strain increment is applied with the motor, the measured force will be less if friction is present. This is because at the start of a cycle, the change in load will not be registered by the load cell as long as the resulting force from the strain increments is lower than the static friction. In this case, if the load is measure with the gauge at the top no change in deformation will occur. The force applied with the actuator will at the start of a cycle not give a strain increment before the force applied exceeds the static friction. But the load cell will still measure an increase in the applied load.

6.3 Creep Deformations under Cyclic Loading

The total deformation during cyclic loading may partially be due to creep, especially if the cyclic load endures for a long period of time and the average shear stiffness is high. Creep deformations are assumed to be caused by the monotonic part of the applied load.

Two triaxial tests, with the approximately identical initial conditions, are evaluated to estimate the creep deformations during a cyclic test. One test was done as a creep test and the other as a cyclic test. The static load applied was equal for both tests. Data for the two tests are presented in Appendix B, a brief summary of the two tests are given in Table 6.1.

Table 6.1: Tests used for calculation of creep

Test Type	**Depth** (m)	τ_{ave} (kPa)	τ_{cyc} (kPa)	**Duration** (h)	ϵ_{tot} (%)
Cyclic	10,7	23	$\pm$ 5	18,5	12,0
Creep	11,1	23	-	47,0	1,9

6.3.1 Results

Figure 6.4 shows the development of strain and pore pressure versus time for the creep test. The undrained creep rate(α_c) is estimated from the linear part of the strain curve in Figure 6.4. Towards the end of the test the strain rate is increasing. It is likely to believe that the increasing pore pressure brings the sample closer to failure and therefor causes the strain rate to increase.

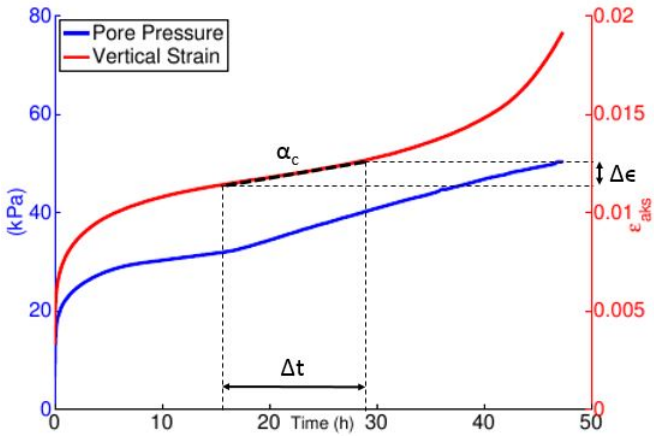

Figure 6.4: Calculation of creep rate

The creep rate is calculated to $7,7 * 10^{-3}$ $mm/h(\frac{\Delta\epsilon}{\Delta t})$. This leads to that 1 % of the total deformation from the cyclic test from 10,7 m is due to creep. This comparison is done for the length of the cyclic test (18,5h).

6.3.2 Conclusion

The deformation due to creep may be neglected for the test from 10,7 m, based on the creep rate calculated.

The pore pressure is increasing in the area where the creep rate is calculated and this will cause a higher degree of mobilization in the soil. More testing has to be done to more accurate determine the creep rate.

6.4 Effect of Degradation

The two samples discussed in Section 6.3 is applied with the same monotonic load, and one of the samples was added a load controlled cyclic amplitude. Compared to the magnitude of the total static load applied, the cyclic amplitude caused a change in the total shear stress to be roughly $\pm$ 10 %. Still the difference in deformation for the two tests is significant. While the sample without the cyclic load had reached 1,2 % deformation after 18,5 h, the test with the cyclic amplitude, for the same period of time, had reached 12 % deformation. The large deformation at the cyclic test has to be a result from the more than just an increased load was applied.

By evaluating the pore pressure, Figure 6.5a, the pore pressure in the cyclic test is increasing more rapidly than the creep test. Figure 6.5b shows how the pore pressure is increasing in the creep test to the same values as the cyclic test. But the total strains is still much lower than the cyclic test. Even though the cyclic amplitude is relative less than the monotonic shear stress, the cyclic load is clearly causing a degradation of the clay structure.

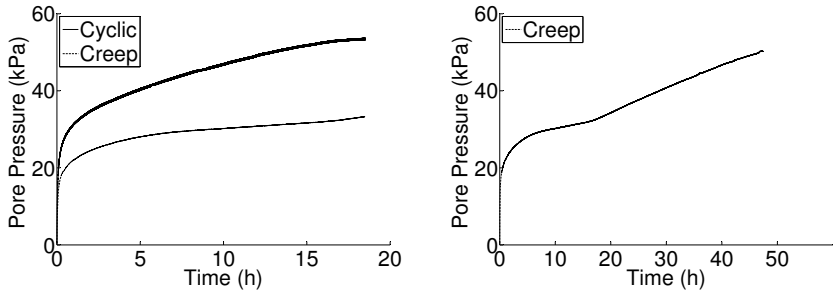

(a) Cyclic and creep (b) Creep

Figure 6.5: Pore pressure development

The strain rate for the test with the constant load increased significantly at the end of the test, ref. Figure 6.4. Still it is highly unlikely that the total strain would be even close to deformation from the cyclic test, even though the test had endured for a longer period of time.

6.5 Undrained Cyclic Shear Strength

The reduction in static capacity caused by a cyclic load is evaluated. A constant rate of strain under undrained conditions was applied some of the triaxial samples after the cyclic loading phase was terminated. An overview of the samples are presented in Table 6.2. All samples where consolidated to a K_0' condition.

Table 6.2: Cyclic phase(es) for samples where the static capacity is found

Depth	**Cyclic phase nr.1**			
	$\boldsymbol{\Delta\sigma}$	$\boldsymbol{\tau_{cyc}}$	**N**	$\boldsymbol{\Delta\epsilon_{aks}}$
(m)	(kPa)	(kPa)	(-)	(%)
10,6	0	± 10	6500	0,4
11,2	46	± 20	126	10,5
11,5	46	± 20	90	11,6
11,6	10	$\boldsymbol{\epsilon_{cyc}} = \pm 75\mu m$	650	-
Depth	**Cyclic phase nr.2**			
	$\boldsymbol{\Delta\sigma}$	**Amplitude**	**N**	$\boldsymbol{\Delta\epsilon_{aks}}$
(m)	(kPa)	(kPa)	(-)	(%)
10,6	20	$\boldsymbol{\tau_{cyc}}=\pm 10$	2500*	1,7
11,2	0	$\boldsymbol{\tau_{cyc}}=\pm 5$	5000	0

*Approximate value

The maximum undrained static capacity (τ_f) of the soil is determined by a shear phase on a sample from 11,4m. A disturbance in this test influenced the pore pressure development. Even though the stress path is affected by this, the maximum capacity is as expected according to the results from Frydenberg et al. (2013).

6.5.1 Result

The shear phase for all samples presented in Table 6.2 and the reference sample from 11,4 m are presented in Figure 6.6.

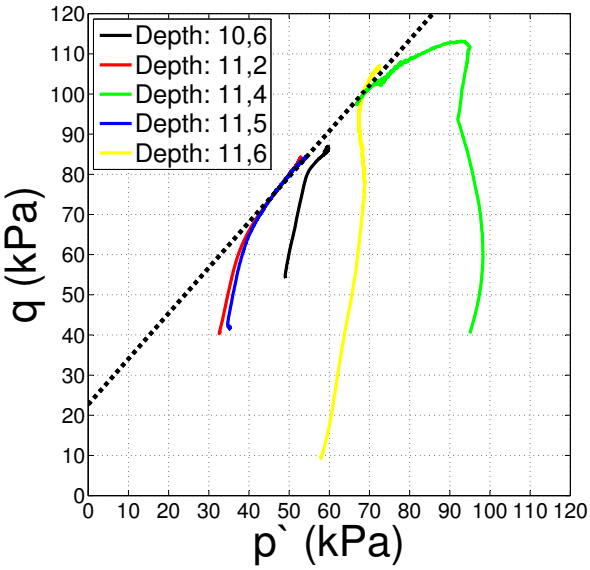

Figure 6.6: Undrained shear strength after cyclic phase, the test from Depth:11,4 is not applied with a cyclic phase

The failure line is plotted with $\phi = 28°$ and a=20 kPa.

6.5.2 Conclusion

When brought to failure by shear, all samples follows the approximate same line of failure.

The sample from 11,2 and 11,5 was postponed for the approximate same stress conditions. The sample from 11,2 was postponed for an extra 5000 cycles. These extra cycles resulted in no extra strain accumulation and only a minor(5 kPa) increase in pore pressure was measured. The undrained cyclic shear strength, for the two samples, is almost identical.

7. Results from Cyclic Modeling

The results from the simulation of a cyclic triaxial test in PLAXIS are obtained from parallel coupling, by an Iwan model, several Cam Clay models. Modeling of the triaxial test is demonstrated in Appendix D.2.1, together with the system of axes used in PLAXIS 2D. Simulation of a triaxial shear phase was done with both user-defined scripts used in this thesis(CCMD and MPS) to see if the calculated results was within acceptable tolerance limits. The triaxial shear test was done using the Soil Test option in PLAXIS 2D 2012. .

7.1 Validation and Evaluation of User-Defined Soil Models

Different parameters used in this validation would have resulted in different calculated values. However the presented values are representative for the most general results and is chosen to highlight any eventual issues that may arise.

7.1.1 Triaxial shear test

Results obtained with the script representing the soil(CCMD) and the script that enables parallel coupling(MPS) has been compared to hand calculated values for two easily defined stress states. Calculations has

been done by simulation of a CIU_c in a triaxial cell, failure is defined at 10 % vertical strain.

Two different scenarios are presented, one highly overconsolidated(OC) and the other is slightly overconsolidated refereed to as NC. The parameters used are presented in Table 7.1.

Table 7.1: Stress states and parameters used for validation of used-defined models

	κ (-)	λ (-)	G (kPa)	e_0 (-)	M (-)	p'_{ini} (kPa)	p'_0 (kPa)	OCR (-)
NC	0,04	0,2	2000	0,5	1,0	240	300	1,25
OC	0,06	0,3	2700	1,0	1,5	60	200	3,33

Each of these problems are also divided into groups, to see if the response of each individual group would sum up to the same result as the original problem. Each group are assigned with the same material set as the respective problem, the stresses are also divided equally among the groups.

Results:
Values calculated by hand compared to the results from the user-defined scripts are presented in Appendix D.1.1 and D.1.2.

Figure 7.1 presents vertical strain vs. applied load, for a problem divided into two(n=2) and three(n=3) groups. The original response(n=1) is also presented.

Conclusion:
Values for the maximum shear stress and pore pressure at failure calculated by the user-defined scripts gave equally results as the values calculated by hand.

By dividing a problem into groups the approximate same failure load is obtained when the groups are assigned with the same material parameters

as the original problem. But the total stiffness in the elastic area will increase as more groups as included. The results from Figure 7.1 shows how the stiffness is increasing by a factor of n.

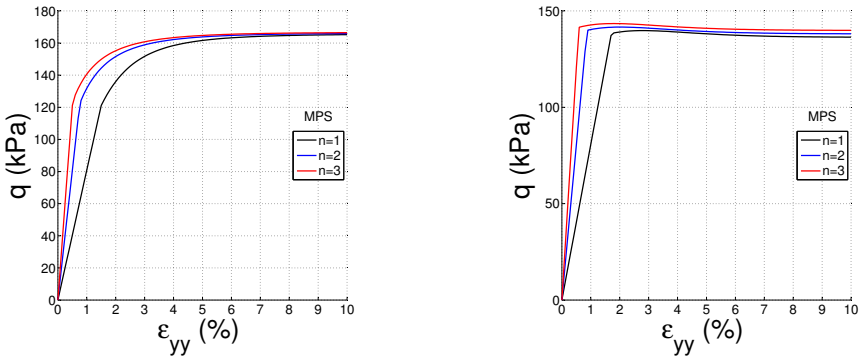

(a) Slightly overconsolidated (b) Highly overconsolidated

Figure 7.1: Change in stiffness according to number of groups included in the Iwan model. Calculated values with the MPS

7.1.2 Cyclic triaxial test

A soil sample, modeled by three sets of material parameters, was postponed for 100 cycles. The response of the system is independent of frequency of the applied load, it is the number of cycles that will have influence on the final result. The response of the material is calculated from two different initial stress conditions, one isotropic (CIU_{cyc}) and one anisotropic(CAU_{cyc}). The stress conditions are presented in Table 7.2.

Table 7.2: Stress conditions for cyclic triaxial validation

	σ_{yy} (kPa)	σ_{xx} (kPa)	$\Delta\sigma_{yy}$ (kPa)
CIU_{cyc}	150	150	± 40
CAU_{cyc}	170	150	± 40

The material parameters used in this simulation are presented in Table 7.3. The difference between these sets is primarily that two of them are assigned with a M value much lower then the set with the highest value.

Table 7.3: Parameters used for cyclic triaxial validation

	κ (-)	λ (-)	G (kPa)	e_0 (-)	M (-)	OCR (-)	x_0 (-)	a_p (-)	a_q (-)
Set 1	0,06	0,4	5500	0,7	0,6	1,1	5	4,5	2,0
Set 2	0,05	0,5	5900	0,5	0,4	1,2	4	4,5	2,0
Set 3	0,06	0,3	4900	0,4	1,2	1,4	5	4,0	1,5

Results:
The results from modeling of the cyclic triaxial tests from the two stress states described by Table 7.2 is presented in Figure 7.2 and 7.3.

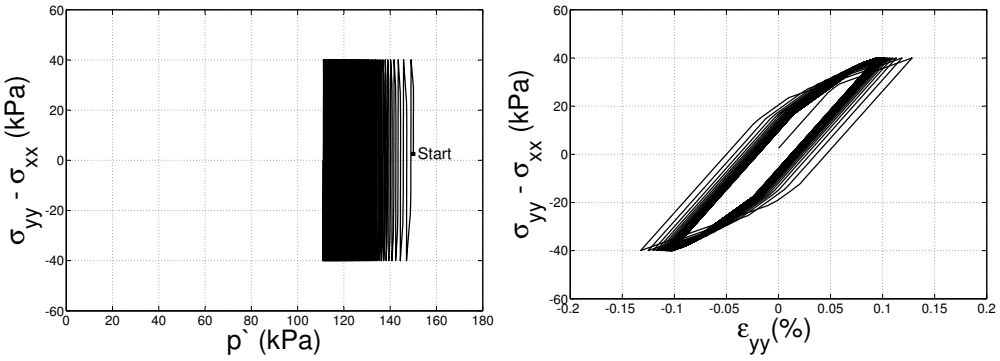

(a) $p' - (\sigma_{yy} - \sigma_{xx})$ (b) $\epsilon_{yy} - (\sigma_{yy} - \sigma_{xx})$

Figure 7.2: Simulation of CIU_{cyc} triaxial test, values obtained from PLAXIS 2D 2012

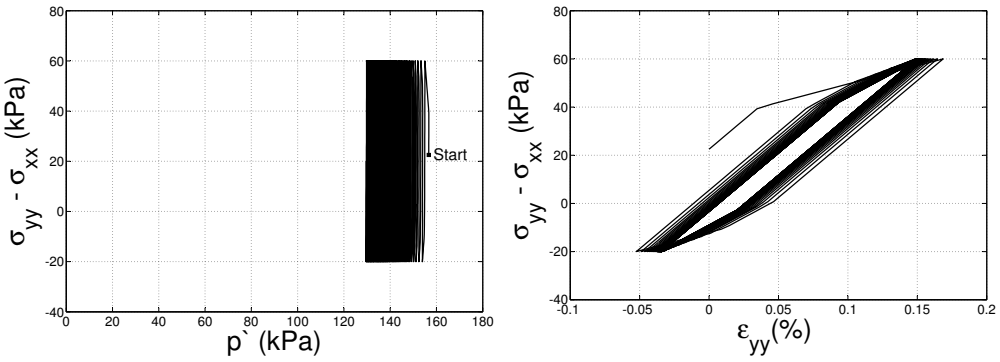

(a) $p' - (\sigma_{yy} - \sigma_{xx})$ (b) $\epsilon_{yy} - (\sigma_{yy} - \sigma_{xx})$

Figure 7.3: Simulation of CAU_{cyc} triaxial test, values obtained from PLAXIS 2D 2012

The average and maximum shear stiffness for the first and last cycle for the two different stress states in Figure 7.2 and 7.3 are presented in Table 7.4.

Table 7.4: Variation in G_{max} and G_{sec} based on Figure 7.2 and 7.3

	Figure 7.2		**Figure 7.3**	
	N_1	N_{100}	N_1	N_{100}
G_{max} (kPa)	16200	16200	17100	17100
G_{sec} (kPa)	10200	12700	12100	14000

Conclusion:
Compared to the cyclic triaxial tests presented in Chapter 6 the calculated results gave a pore pressure build-up that seems reasonable. The pore pressure is increasing more rapidly at the start of the test and stabilizes after a time. The magnitude of the pore pressure should probably have been a little higher based on the applied load and stress condition, this could be accounted for by increasing the constants controlling the degradation.

Based on the stress condition and the cyclic triaxial tests from Chapter 6, the calculated strain for the simulated CAU_{cyc} triaxial test should have been up by a factor of 50 or more. It was also expected the G_{sec} value to decrease, but a slightly increase has been calculated. As a result from the low accumulated strain and the development of the average stiffness the hysteresis loops follows the approximate the same path for each cycle.

Both the unloading and reloading path in the strain stress diagrams shows a stiffness behavior as expected according to theory from the Iwan model. Three set of different parameters included, and two different stiffnesses are observed. The calculated G_{max} values compares good to the total shear modulus included.

7.2 Further Evaluation of the Cyclic Results

The simulation of a CAU_{cyc} triaxial test in Section 7.1.1 resulted in almost neglectable accumulated strains. This section addresses how the plastic strains might be increased.

Development of plastic strains will, for undrained conditions in the Cam Clay Model, be dependent of elastic strains. Basic elastic theory states that if the stiffness is reduced, the strains will increase. Parameters affecting the elastic volumetric strain, with respect to the input parameters in the implemented Cam Clay Model are given by the equation for the bulk stiffness:

$$K = G\,\frac{2(1+\nu)}{3(1-\nu)} \tag{7.1}$$

The shear modulus is assumed constant throughout the calculation and by a reduction in G a reduced bulk stiffness will follow.

7.2.1 Methods of solution

Two methods of addressing the problem of low accumulated plastic strains are presented:

- ***Decrease the total stiffness:*** Decreasing the shear stiffness equally at all groups in the included parameters set.
- ***Assign stiffness according to strength:***The idea is to assign a lower shear modulus to the stronger material set and a higher shear modulus to the weak groups. As the weak groups starts yielding and fails, the stiffness will be reduced and this will cause an increase to the plastic strains. The total elastic shear modulus will remain constant.

7.2.2 Results

The results of lowering the shear modulus are shown in Figure 7.4. The parameters used are similar to the parameters in Table 7.3, the difference is that the shear modulus(G) at each model is reduced by 3 000 kPa.

Adjusting the shear modulus to get an increased in the plastic strain was not successfully done when three set of parameters was included into the model. The desirable behavior was more easily obtained as more set of parameters was included into the model. The presented result, Figure 7.5, includes 10 sets of parameters.

The parameters chosen for both cases are presented in Appendix D.2.2. As a remark, the total elastic shear modulus for the values used to calculate the results in Figure 7.5 is chosen to a high value compared to the other simulations.

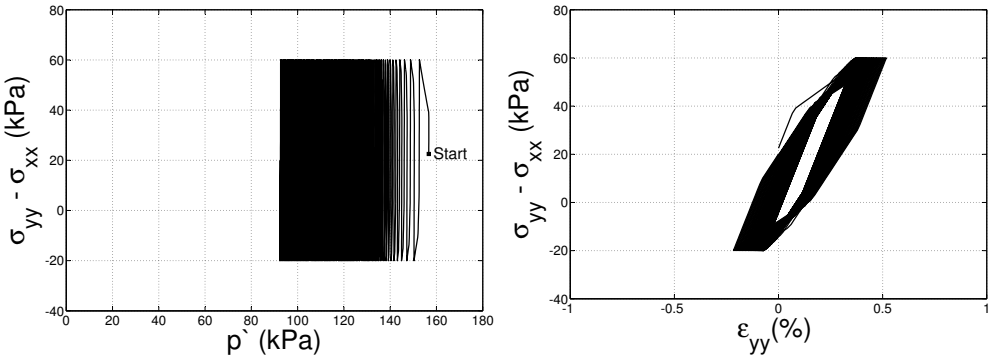

(a) $p' - (\sigma_{yy} - \sigma_{xx})$ (b) $\epsilon_{yy} - (\sigma_{yy} - \sigma_{xx})$

Figure 7.4: CAU_{cyc} triaxial test: Shear modulus decreased equally at all set of parameters

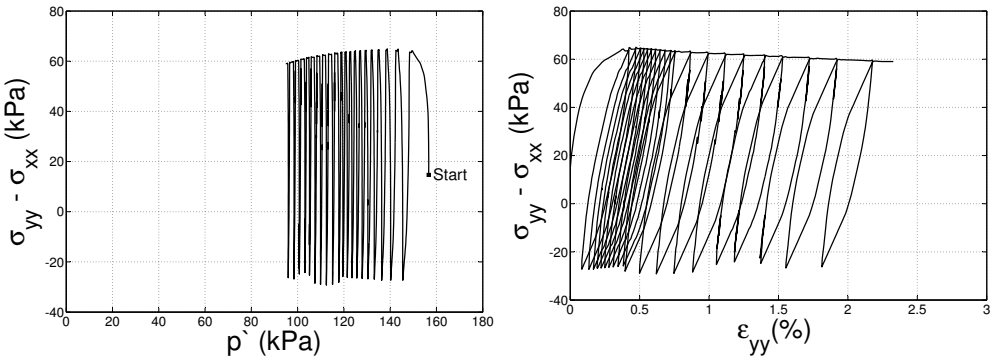

(a) $p' - (\sigma_{yy} - \sigma_{xx})$ (b) $\epsilon_{yy} - (\sigma_{yy} - \sigma_{xx})$

Figure 7.5: CAU_{cyc} triaxial test: Shear modulus distributed according to strength in the included parameters set

Table 7.5 shows how the G_{sec} and G_{max} value varies through the cyclic results in Figure 7.4 and 7.5. The simulation in Figure 7.5 was aborted after 20 cycles.

Table 7.5: Variation in G_{max} and G_{sec} based on Figure 7.4 and 7.5

	Figure 7.4		**Figure 7.5**	
	N_1	N_{100}	N_1	N_{20}
G_{max} (kPa)	2400	2400	20600	20400
G_{sec} (kPa)	1500	1200	9000	7800

7.2.3 Conclusion

In both simulations the average shear stress decreases. For the results presented to be realistic, a larger decrease was expected.

By equally lowering the shear modulus, a significant increase in the accumulated strain is not observed. But an increase in the cyclic strain is obtained.

When the shear modulus is distributed according to strength, the accumulated strain approaches a more realistic value. However there are some new problems that have to be closer evaluated. The applied load in the simulation should have changed as an even sine function, with the maximum and minimum value equal for each cycle. The horizontal load is neither constant through the simulation. An unknown error aborted the simulation after 20 cycles. Vertical -and horizontal load as a function of time is added in Appendix D.2.2.

It may look like the sample area is change during the calculation. In the dynamic calculation phase in PLAXIS 2D 2012, updated mesh can not be taken into account Plaxis (2012b), so the problem do not lies in that there is a change in sample area.

8. Analysis & Discussion

The model that has been developed is able to simulate some of the undrained cyclic response of clay with realistically results. There is still some challenges that have to be solved for the cyclic model to work properly. Improvements to the triaxial testing device are also necessary if further cyclic tests is to be conducted. A thoroughly analysis to highlight the challenges from the numerical simulations and triaxial tests are evaluated in the first two sections of this chapter.

The last section addresses the issues that have to be solved to strengthen the model for further development.

8.1 Numerical Modeling of Cyclic Behavior

The primary focus in the evaluation of the calculated results was in the interaction between pore pressure build-up, hysteresis effect and development of permanent strains. The magnitude and ratio between the pore pressure and permanent strains expected from the calculated results are based on the experience gained from the triaxial testing. A simulation where all three of these effects have resulted in realistically values at the same time has not successfully been done. Based on the most common results from the cyclic triaxial simulations realistic development of pore pressure is possible. But the combination of low accumulation of plastic strains and a G_{sec} value only slightly changing resulted in hysteresis loop almost identical through the simulation.

The response of the system fully depends on values of the parameters included and the interaction between these. And infinite number of pa-

rameters may be chosen into the model and an equal number of solutions are possible. The groups of parameters included into the model have to be determined manually by the user. As more and more groups are included into the model, each assigned with its unique set of parameters, the interaction between the parameters makes it harder to obtain the desirable response. A typical response of the system, if a bad combination of parameters are chosen, is either an elastic behavior after the first cycle or a numerical error at the start of the cyclic phase.

8.1.1 Pore pressure

Modeling realistically values and build-up for the pore pressure for undrained cyclic loading have been done, by the right combination of parameters. The pore pressure was in general found to increase more rapidly at the start of the test and a stabilized value was reached after sufficient number of cycles had been modeled.

8.1.2 Hysteresis

Including several groups with different parameters allows for a behavior which look a lot similar like a rounded hysteresis loop. This effect has clearly be shown in Section 7.1.2. However the presented hysteresis loops are almost identical for the whole simulation because of low value of the accumulated strain and only sligh change in stiffness.

Combination of parameters that account for pore pressure build-up will also cause hysteresis loops. The author has not been able to model one effect without the other also was included. If too high strength parameters are assigned, none of the models will fail and the response of the system will be totally elastic.

8.1.3 Accumulated strain and change in stiffness

Determination of parameters to model a realistic development of accumulated strains and change in stiffness has been found hard.

Plastic strains:
The attempt to increase the plastic strains where the shear modulus was distributed according to strength of the included material sets, presented in Section 7.2, is further analyzed. The basis for this solution is that for undrained conditions in the soil model that was used, elastic and plastic strains are related. This solution resulted in an increase in the plastic strains by the number of cycles. It also caused the average stiffness to decrease. The downside is that it caused some new problems that have to further be evaluated:

- The response from the vertical and horizontal load was not as expected. The applied load in the simulation did not changed as an even sine function, neither was the maximum and minimum value equal for each cycle. The horizontal load did vary through the simulation, this value should have remained constant. Vertical -and horizontal load as a function of time is added in Appendix D.2.2.
- The simulation did come to a stop after a number of cycles(N$\sim$ 20) had been calculated.
- The calculation time for each cycle was up by a factor of 100. The global error did also increase.

As a remark: None of the problems listed above was present when the elastic shear modulus was equally distributed among each group. But then the calculated plastic strain was too low.

The increase in the plastic strain that contributed most to the accumulation of strains is when the last and strongest material set was yielding. The shape of the strain stress curve, Figure 7.5, is not be regarded as realistic. If the listed problems above are solved, the model would likely describe

the general trend regarding the soil response from cyclic loading.

Stiffness:
The G_{max} calculated may be regarded as constant in the simulation in the results presented. This is as expected from theory of the Iwan model. A reduction in the average stiffness was observed when the shear modulus was adjusted, Section 7.2. In the results from Section 7.1.2 the G_{sec} value increased. The change in stiffness most likely depends of the interaction between the parameters included.

Creep deformations:
Deformations under constant monotonic load is not accounted for by the included model. The results from the triaxial tests concluded that creep was neglectable for the total deformations for the time ($t \sim 20h$) and stress condition evaluated.

8.2 Triaxial Tests

High quality testing is essential if the results from triaxial tests are to be combined with numerical modeling. This implies that the user has to have control over the components that may cause a deviation to the results.

The results from Section 6.2 showed that the friction between the load rod and the triaxial testing device may easily affect the results and the user has low control over this while the test is running. Modifications should be done to make sure the friction do not inflicts with the measured results. Separate the energy loss between friction and hysteresis is not possible since the friction is a function of varying parameters that may not be determined numerically.

8.2.1 Modifications

Initially the load rod should be perfectly centric down in the hole in the triaxial cell. It may seem that the friction comes from that the rod gets tilted and/or horizontally displaced after it has been mounted into the top piece. It is difficult to see if the rod has moved during the test, and it is hard to prevent this as the device is build today. Therefore a solution where the tilting of the soil sample and the top piece don't afflict the orientation of the rod is sought.

Three different solutions are presented, a combination between these three are also possible:

Tripod:
This solution would make the top piece independent of the tilting of the soil sample so it only follows the vertical displacement of the sample. The top piece will stay horizontal and centric inside the cell.

The top piece rests a top of the sample, but is mounted to three vertical "legs". The top piece may then slide up and down this legs according to the vertical deformation of the sample. The solution is shown in Figure 8.1a. Holes, with threads, for the legs have to be drilled into the bottom plate.

The sliding may cause friction in the system and the requirement of high precision in the installation of the legs may be hard to accomplish.

Modify the top piece:
This solution would make the any displacement of top piece independent of the load rod.

One way to do this is to plug the hole in the top piece. The rod and the top piece can be connected, e.g. by a ball, which allows for no horizontal forces to be transmitted, illustrated in Figure 8.1b.

The downside with this solution is if movement of the top piece gets the ball of center, the transition between the rod and the ball is lost. The test then has to be terminated.

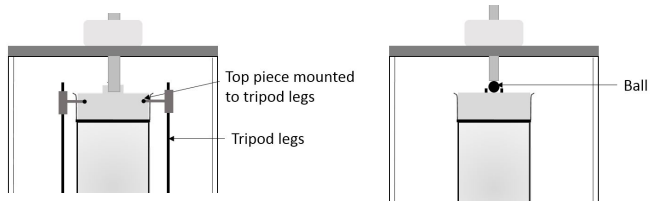

(a) Tripod (b) Top Piece

Figure 8.1: Recommended modifications of the triaxial cell

Move the load cell:
The easiest solution is to place the load cell inside the triaxial cell. The friction will still be present, but the measured values will reflect the force which are applied to the sample. Placing the load cell inside the triaxial cell, requires a new triaxial cell with an increased height.

8.2.2 Corrected area

The corrected area(A_s) in a triaxial test is calculated by the expression:

$$A_s = \frac{A_a}{1 - \epsilon_{aks}} \tag{8.1}$$

where A_a is the area of the sample after consolidation.

Eq. (8.1) assumes that the geometry of the sample always will be a cylinder. As the deformations increases this assumption is less valid. Results showed that at high deformation the samples in general deformed more around the middle and in some cases the top piece was pushed down into the sample. The stresses in the sample will therefore vary. At high strains a uniform stress distribution through the sample will not reflect the reality.

A picture should have been taken of the sample after each test had finished. The accuracy of the calculated values could therefore had been evaluated more thoroughly.

8.3 Improvements

One possible way to obtain the parameters need for an accurate simulation of the cyclic behavior of the soil is to obtain the values from a cyclic triaxial test preformed on a representative soil sample. A mathematical algorithm could be used to find the parameters that would give the best match between the cyclic test and the modeled result. The values obtained could be verified by back calculating another cyclic triaxial test.

If values are to be obtained from a triaxial test, high quality testing are essential. This demands that all factors that will contribute to a deviation has to come under control. For the triaxial device used in this thesis, the main problem is the friction force between the load rod and triaxial cell. With the proper modifications the influence of the friction can be reduced. It is also recommended that further triaxial testing is done with use of back pressure, to reduce the influence of air bubbles in the system. Even with the modifications the quality of the tests is highly dependent on the operator.

Cyclic loading in PLAXIS are calculated in the dynamic phase, which do not account for updated mesh. This implies that the applied load is constant through the simulation since the sample area do not change. In the triaxial device the vertical stress are reduced through the cyclic phase since the area of the sample is increasing. A possible way to solve this is to describe the applied load in PLAXIS by an implemented text file, which accounts for a reduction in the applied load. Other possibilities are to updated the geometry in PLAXIS by selecting a new calculation phase. This option is limited due to practical reasons. Modification of the software used for the triaxial testing may be done to account for updated area.

9. Conclusions and Recommendations for Further Work

9.1 Summary and Conclusions

Undrained cyclic response of clay has been simulated by an Iwan model combining several elasto-plastic soil models coupled in parallel. Each of these models was assigned with a unique set of parameters. A great advantage of using Iwan models is that all parameters needed are only related to the soil models included. The cyclic model is independent of mass and damping which implies that the model is not dependent of frequency of the applied load. The Cam Clay Model is used to describe the soil behavior, degradation of the soil structure is included into the model.

Seven triaxial tests have been conducted. Five of these were cyclic tests, all with a different amplitude. Initially the thought was to back-calculate one of the triaxial tests. This have not been done because determination of parameters was found to be a time-consuming process. The triaxial tests rather made basis for the improvements of the cyclic model. High friction forces was found to disturb the quality of the cyclic tests.

Based on the most common results from the triaxial simulations, a realistic pore pressure build-up may be modeled. Hysteresis in the soil will also be accounted for. However, low accumulation of plastic strains and only a slight change in stiffness resulted in approximate identical hysteresis loops calculated for each cycle. The reason for this is most likely that the right value, number and interaction between the included parameters

have to be found. There are some unsolved issues regarding modeling of the permanent strain that have to further be evaluated. By solving these problems, this method is likely to be representative for the general trend during undrained cyclic loading of clay if correct parameters are included.

9.2 Further Work

Manually determination of parameters is a time consuming process and there is no guarantee of a realistic results. By using a mathematical algorithm the value and number of parameters could be determined automatic from a cyclic triaxial test. The quality of the values obtained could be validated by back-calculation of a similar cyclic test.

High quality of the triaxial tests are necessary if they should be used in combination with the numerical modeling. Friction forces are also found to disturb the results. The triaxial cell should be modified before any more testing are done. It is recommended that further testing is done with back pressure to further increase the quality of the tests.

Bibliography

K. H. Andersen. Bearing capacity under cyclic loading -offshore, along the coast, and on land. *Can. Geotech Journal*, 46:513–535, 2009.

R. D. Cook, D.S Malkus, M. E. Plesha, and R.J. Witt. *Conceepts and Applications of Finite Element Analysis*. Hamilton Printing Company, fourth edition, 2002.

Olav Frydenberg, Henning Firman, and Christofer Klevsjø. TBA 4110 Hovedrapport. Technical report, NTNU, 2013.

G. Grimstad, J.A. Rønningen, and H.A. Nøst. Use of IWAN models for modelling anisotropic and cyclic behavior of clays. pages 1–6, 2014.

K.H. Head. *Manual of Soil Laboratory Testing*. Pentech Press Limited, London, 1986.

G. T. Houlsby and A. M. Puzrin, editors. *Principles of Hyperplasticity*. Springer, Oxford, 2006.

T.J.R Hughes. *The Finite Element Method Linear Static and Dynamic Finite Element Analysis*. Dover Publications, Inc., Mineola, New York, 2000.

Steven L. Kramer. *Geotechnical Earthquake Engineering*. Prentice Hall, Uppper Saddle River, New Jersey, 2010.

S. Nordal. *SOIL MODELING Lecture notes PhD course BA8304*. NTNU, Trondheim, 2012.

S. Nordal. *TBA 4116 Geotechnical Engineering Advanced course.* Kompendieforlaget, Trondheim, 2013.

Plaxis. *PLAXIS Material Models Manual 2012*, 2012a.

Plaxis. *PLAXIS 2D Reference Manual 2012*, 2012b.

Plaxis. *PLAXIS Scientific Manual 2012*, 2012c.

R. Sandven, Senneset K, A. Emdal, S. Nordal, N. Janbu, L. Grande, and H. A. Kornbrekke. *Geotechnics Field and Laboratory Investigations.* NTNU, Trondheim, 2013.

D. M. Wood, editor. *Soil Behaviour and Critical State Soil Mechanics.* Cambridge University Press, Cambridge, 1990.

List of Figures

2.1 Stress path for an elastic perfectly plastic model, after Nordal (2013) . . . 9
2.2 Critical State . . . 15
2.3 Stress path undrained loading Cam Clay . . . 16
2.4 Softening in the Cam Clay model . . . 17

3.1 Shear strain during cyclic loading Andersen (2009) . . . 20
3.2 Cyclic and monotonic shear stress after Andersen (2009) . . 22
3.3 Series coupling of an Iwan model, after Houlsby and Puzrin (2006) . . . 24
3.4 Parallel coupling of an Iwan model . . . 25

4.1 Flow chart of parallel coupling in PLAXIS . . . 28
4.2 Effect of the degradation constants in the UD Cam Clay model . . . 32
4.3 Undrained cyclic loading of a soil model with degradation included . . . 33
4.4 Cyclic stress path and stiffness, after Houlsby and Puzrin (2006) . . . 35

5.1 Triaxial test device used . . . 40

6.1 Areas where friction occurs . . . 44
6.2 Cyclic loading of a rubber sample . . . 45

6.3 Friction from two cyclic triaxial tests 46
6.4 Calculation of creep rate 48
6.5 Pore pressure development 50
6.6 Undrained shear strength after cyclic phase, the test from Depth:11,4 is not applied with a cyclic phase 52

7.1 Change in stiffness according to number of groups included in the Iwan model. Calculated values with the MPS 55
7.2 Simulation of CIU_{cyc} triaxial test, values obtained from PLAXIS 2D 2012 57
7.3 Simulation of CAU_{cyc} triaxial test, values obtained from PLAXIS 2D 2012 57
7.4 CAU_{cyc} triaxial test: Shear modulus decreased equally at all set of parameters 61
7.5 CAU_{cyc} triaxial test: Shear modulus distributed according to strength in the included parameters set 61

8.1 Recommended modifications of the triaxial cell 68

C.1 Depth 11,2: Cyclic pore pressure and shear strain vs. average values 106
C.2 Depth 11,5: Cyclic pore pressure and shear strain vs. average values 107
C.3 Depth 11,6: Cyclic pore pressure and shear strain vs. average values 108

D.1 An isotropic stress state described by two independent models 111
D.2 Stress path, undrained Cam Clay 113
D.3 Triaxial device in PLAXIS and system of axis 114
D.4 Change in vertical load, shear modulus distributed according to strength of the parameters 116
D.5 Change in horizontal load, shear modulus distributed according to strength of the parameters 116

List of Tables

3.1 Frequencies at given situations Head (1986) 19

4.1 Input parameters for the user-defined Cam Clay Model . . . 31

5.1 Sample quality based on expelled water Sandven et al. (2013) 39

6.1 Tests used for calculation of creep 48
6.2 Cyclic phase(es) for samples where the static capacity is found 51

7.1 Stress states and parameters used for validation of used-defined models 54
7.2 Stress conditions for cyclic triaxial validation 56
7.3 Parameters used for cyclic triaxial validation 56
7.4 Variation in G_{max} and G_{sec} based on Figure 7.2 and 7.3 . . 58
7.5 Variation in G_{max} and G_{sec} based on Figure 7.4 and 7.5 . . 62

B.1 Overview of the triaxial tests conducted 87
B.2 Parameters regarding the soil and site at Stjørdal, from Frydenberg et al. (2013) 88
B.3 Consolidation values. Depth: 10,6m 90
B.4 Consolidation values. Depth: 10,7m 92
B.5 Consolidation values. Depth: 11,1 94
B.6 Consolidation values. Depth: 11,2m 96
B.7 Consolidation values. Depth: 11,4m 98

B.8 Consolidation values. Depth: 11,5m 100
B.9 Consolidation values. Depth: 11,6m 102

C.1 Tests where cyclic pore pressure and shear strain are shown 105
C.2 Depth 11,2: Initial shear stress and load amplitude 106
C.3 Depth 11,5: Initial shear stress and load amplitude 107
C.4 Depth 11,6: Shear stress and strain amplitude 108

D.1 Scenarios used for validation of used-defined models 109
D.2 Results Cam Clay w/ Degradation 110
D.3 Results MPS 112
D.4 Lower the shear modulus equal in all sets 115
D.5 Distribution of shear modulus according to strength 115

List of Symbols Abbreviations

Abbreviations & Terms

CAU_{cyc}	Anisotropic consoildation, undrained cyclic test
$CCMD$	Cam Clay Model with Degradation
CIU_c	Isotropic consoildation, undrained compression test
CIU_{cyc}	Isotropic consoildation, cyclic undrained test
CSL	Critical State Line
ESP	Effective Stress Path
FEM	Finite Element Method
GWL	Ground water level
kPa	kilo Pascal (pressure)
MPS	Script which enables parallel coupling of a soil model
NC	Normally consolidated
$NTNU$	Norwegian University of Science & Technology
OC	Overconsolidated
OCR	Over Consolidated Ratio
$PLAXIS$	FEM Program for Geotechnical Engineering
TSP	Total Stress Path
UD	User-defined

Roman Letters & Symbols

a	Attraction
A_0	Initial area
A_a	Area after consolidation
a_p	UD parameter in CCMD controlling degradation
a_q	UD parameter in CCMD controlling degradation
A_s	Updatet area
D	Spring stiffness
d	infinitesmall increment
$d\lambda$	Plastic multiplier
$\boldsymbol{D_e}$	Elastic stiffness matrix
$\boldsymbol{D_{ep}}$	Total stiffness matrix
e	void ratio
E	Elastic modulus
G	Shear modulus
G_{max}	Maximal shear modulus
G_{sec}	Average shear modulus
G_{tan}	Tangential shear modulus
h	Height
h	Hours
Hz	Frequency
I_L	Liquidity index
I_P	Plasticity index
K	Bulk Modulus
K_0'	Earth pressure coefficient at rest
L_i	Initial length of spring
M	Inclination of Mohr–Coulomb surface in p'-q-plot
N	Number of cyclic loops
n	number of groups in the Iwan model
N_i	Cycle nr i
p'	Effective Volumetric stress
p_0'	Isotropic preconsolidation
p_c'	Anisotropic preconsolidation
p_{ini}'	Initial preconsolidation stress
Q	Plastic potential
q	Deviatoric stress
q_f	Deviatoric stress at failure
u	Total pore pressure
u_{cyc}	Cyclic pore pressure
u_0	Average pore pressure
v	Specific volume
V_0	Initial volume
v_0	Initial specific volume
w	Water content
x_0	UD parameter in CCMD controlling degradation

Greek Letters & Symbols

α_c	Creep rate	ν	Poisson's ratio
Δ	Finite increment	ϕ	Friction angle
ϵ	Strain	σ	Stress
ϵ^e	Elastic strain	σ_1	Maximum total principal stress
ϵ^p	Plastic strain		
ϵ_{aks}	Vertical strain	σ'_1	Maximum effective principal stress
ϵ_{cyc}	Cyclic strain amplitude		
ϵ_q	Deviatoric strain	σ_3	Minimum total principal stress
ϵ_q	Volumetric strain		
ϵ_{tot}	Total volumetric strain	σ'_3	Minimum effective principal stress
ϵ_{vol}	Volumetric strain		
ϵ_{yy}	Vertical strain in PLAXIS	σ_{xx}	Cartesian normal total stress in x-direction
γ	Sear strain		
γ_{ave}	Average shear strain	σ_{yy}	Cartesian normal total stress in y-direction
γ_{cyc}	Cyclic shear strain		
κ	Flexibility constant OC, Cam Clay	τ	Shear stress
		τ_{ave}	Average shear stress
κ	Hardening parameter	τ_{cyc}	Cyclic load amplitude
λ	Flexibility constant NC, Cam Clay	τ_{tot}	Total shear stress
		ξ	Damping ratio

A. Text of Thesis

NTNU
Faculty of Engineering Science and Technology
Institute of Civil and Transport Engineering

MASTER DEGREE THESIS

Spring 2014
for

Student: Christofer Klevsjø

Numerical Modeling of Cyclic Loading on Clay
Numerisk modellering av sykliske laster på leire

BACKGROUND

There is currently no commercial software that offers a soil model that is able to accurately model cyclic loading on clay. One "simple" and pragmatic way to model undrained behavior of soil subjected to cyclic loading is to combine several elasto-plastic soil models in parallel or series (Iwan type of model). Hysteresis effect and pore pressure build-up could then be taken into account. The soil behavior under cyclic loading, e.g. earthquakes, may then be more accurate estimated.

TASK

Task description
Create a simple formulation that is able to describe the overall behavior of undrained cyclic loading on clay, within the effective stress concept. The overall task is split in three subtasks. 1st task is to get acquainted with the theory, 2nd task is to do the modelling/implementation and 3rd is validation.

Objective and purpose
Create a user- defined script which is able to parallel couple a soil model (Cam Clay with destructuration). This script shall be used to simulate the effect cyclic loading causes on clay. The results from the simulation shall be compared to triaxial tests.

Subtasks and research questions

The theory part shall contain the basis for the calculations, results and assumptions made in this thesis. Theory describing how the Cam Clay Model works for undrained loading and the factors affects undrained cyclic loading should be explained.

Couple the Cam Clay Model in parallel: A user-defined script is to be made to enable parallel coupling of a soil model. The candidate is to be handed a user-defined script to represent the behavior of a single Iwan element (i.e. Cam clay with destructuration). Calculation with the parallel coupled soil model should be done by the Finite Element Program PLAXIS. Implementation of the new user-defined script into PLAXIS is done by coding in FORTRAN.

Undrained Cyclic Triaxial Tests: Use these results to validate the calculated results. A creep triaxial test should also be done, to see how deformations under constant load affect the results. The triaxial device that shall be used should be presented, with its features. Any factors that may influence the experiment should be described. The setup for this thesis should follow the guidelines from NTNU. All assumptions made, along with the results and conclusion is to be clearly documented.

Is the parallel coupled model able to simulate the response of clay subjected to cyclic loading?

General about content, work and presentation

The text for the master thesis is meant as a framework for the work of the candidate. Adjustments might be done as the work progresses. Tentative changes must be done in cooperation and agreement with the professor in charge at the Department.

In the evaluation thoroughness in the work will be emphasized, as will be documentation of independence in assessments and conclusions. Furthermore the presentation (report) should be well organized and edited; providing clear, precise and orderly descriptions without being unnecessary voluminous.

The report shall include:

- Standard report front page (from DAIM, http://daim.idi.ntnu.no/)
- Title page with abstract and keywords.(template on: http://www.ntnu.no/bat/skjemabank)
- Preface
- Summary and acknowledgement. The summary shall include the objectives of the work, explain how the work has been conducted, present the main results achieved and give the main conclusions of the work.
- The main text.
- Text of the Thesis (these pages) signed by professor in charge as Attachment 1.

The thesis can as an alternative be made as a scientific article for international publication, when this is agreed upon by the Professor in charge. Such a report will include the same points as given above, but where the main text includes both the scientific article and a process report.

Advice and guidelines for writing of the report is given in "Writing Reports" by Øivind Arntsen, and in the departments "Råd og retningslinjer for rapportskriving ved prosjekt og masteroppgave" (In Norwegian) located at http://www.ntnu.no/bat/studier/oppgaver.

Submission procedure

Procedures relating to the submission of the thesis are described in DAIM (http://daim.idi.ntnu.no/). Printing of the thesis is ordered through DAIM directly to Skipnes Printing delivering the printed paper to the department office 2-4 days later. The department will pay for 3 copies, of which the institute retains two copies. Additional copies must be paid for by the candidate / external partner.

On submission of the thesis the candidate shall submit a CD with the paper in digital form in pdf and Word version, the underlying material (such as data collection) in digital form (e.g. Excel). Students must submit the submission form (from DAIM) where both the Ark-Bibl in SBI and Public Services (Building Safety) of SB II has signed the form. The submission form including the appropriate signatures must be signed by the department office before the form is delivered Faculty Office.

Documentation collected during the work, with support from the Department, shall be handed in to the Department together with the report.

According to the current laws and regulations at NTNU, the report is the property of NTNU. The report and associated results can only be used following approval from NTNU (and external cooperation partner if applicable). The Department has the right to make use of the results from the work as if conducted by a Department employee, as long as other arrangements are not agreed upon beforehand.

Tentative agreement on external supervision, work outside NTNU, economic support etc.
Separate description is to be developed, if and when applicable. See http://www.ntnu.no/bat/skjemabank for agreement forms.

Health, environment and safety (HSE) http://www.ntnu.edu/hse
NTNU emphasizes the safety for the individual employee and student. The individual safety shall be in the forefront and no one shall take unnecessary chances in carrying out the work. In particular, if the student is to participate in field work, visits, field courses, excursions etc. during the Master Thesis work, he/she shall make himself/herself familiar with "Fieldwork HSE Guidelines". The document is found on the NTNU HMS-pages at http://www.ntnu.no/hms/retningslinjer/HMSR07E.pdf

The students do not have a full insurance coverage as a student at NTNU. If you as a student want the same insurance coverage as the employees at the university, you must take out individual travel and personal injury insurance.

Startup and submission deadlines
Startup for this thesis is January 15th 2014. The thesis should be submitted electronically in DAIM before June 11th 2014.

Professor in charge: Gustav Grimstad

Department of Civil and Transport Engineering, NTNU
Date: 15.01.2014, (revised: 06.06.2014)

Professor Gustav Grimstad

B. Triaxial Test Results

B.1 Overview of the triaxial results

An overview of the triaxial tests conducted are presented in Table B.1. The sample quality at each test is estimated based on Table 5.1.

All phases, except consolidation, are done undrained and the frequency of the applied load was set to 0,1 Hz. If not else specified the cyclic phases are load controlled.

Table B.1: Overview of the triaxial tests conducted

Depth (m)	**Sample Quality** -	**Test Type** -
10,6	Disturbed	Cyclic and Shear
10,7	Acceptable	Cyclic
11,1	Acceptable	Creep
11,2	Acceptable	Cyclic and Shear
11,4	Acceptable	Shear
11,5	Acceptable	Cyclic and Shear
11,6	Disturbed	Cyclic(strain) and shear

All samples are taken from Stjørdal. Information of the cite and geotechnical parameters are obtained from Frydenberg et al. (2013). Some parameters from this rapport are presented in B.2.

From roughly 3 meters below the surface the soil is described at clayey silt, with increasing content of clay with depth. The soil samples tested in this thesis are from 9-12 meters depth. It is marine clay, and not classified

as quick Frydenberg et al. (2013).

Table B.2: Parameters regarding the soil and site at Stjørdal, from Frydenberg et al. (2013)

GWL (m)	$\boldsymbol{K_0'}$ (-)	$\boldsymbol{\gamma}$ ($\frac{kN}{m^3}$)	**w** (%)	$\boldsymbol{I_L}$ (-)	$\boldsymbol{I_P}$ (%)	$\boldsymbol{\phi}$ °	**a** kPa
2,3	0,7	18,5	20	63	19	26,5	20

B.1.1 Presentation of the Test Results

All triaxial test is presented with the following plots:

- $p' - q$
- $\epsilon_{aks} - q$
- NTNU, $\sigma_3' - \tau$
- NGI, $(\sigma_1' + \sigma_3')/2 - \tau$

Some tests does also have shear strain and pore pressure as a function of time and number of cycles.

Boxed Plot:
For an easier interpretation, the NTNU and NGI plot is presented as boxed plot. This means that a number of cycles has been grouped and is drawn as a square box. The number of cycles that have been grouped varies, from test to test and may also change during a single test. The number of cycles is only marked at the NTNU plot, but the same number is chosen in the NGI plot.

After the consolidation cell pressure is kept unchanged. Change in shear stress comes for change in applied vertical load. All load applied after consolidation is applied under undrained conditions.

B.2 Stjørdal: Depth 10,6 meter

This test was conducted with the following steps:

- **Step 1:** Consolidated to K_0' condition (K_0'=0,7)
- **Step 2:** τ_{cyc} set to ±10 kPa for 12 h
- **Step 3:** $\Delta\tau_{ave}$ + 10 kPa, τ_{cyc} ± 10 kPa. This step endured for 13,5 h
- **Step 4:** Shear phase: Constant rate of strain 1,5 %/h

Table B.3 shows reached values at end of consolidation

Table B.3: Consolidation values. Depth: 10,6m

σ_v' (kPa)	σ_h' (kPa)	τ_{ave} (kPa)	ϵ_{vol} (%)
112,7	77,6	17,6	4,8

Comment

During step 3, the computer logging stopped for 30 min. Based on the data saved before and after this happened, the change during this period may be predicted. During step 3 there are also some irregular sign in the pore pressure and shear strain curve. This likely due to friction in the system.

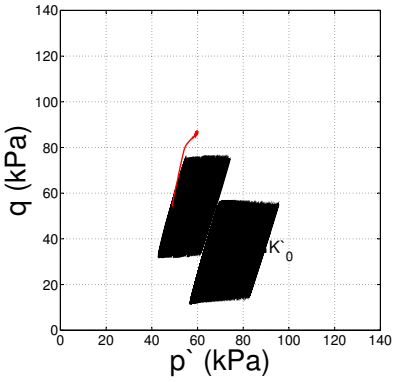
q (kPa)
p` (kPa)
K`0

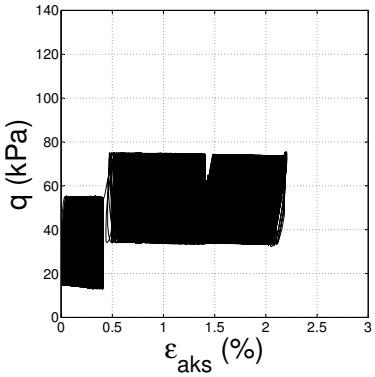
q (kPa)
εaks (%)

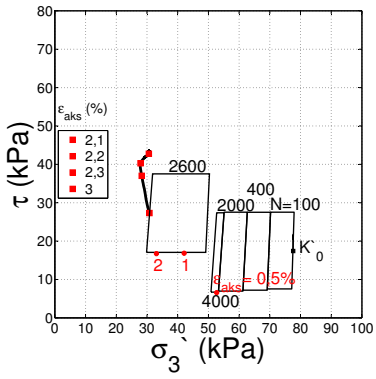
τ (kPa)
σ3` (kPa)
εaks (%)
2,1
2,2
2,3
3
2600
400
2000
N=100
K`0
2
1
εaks= 0,5%
4000

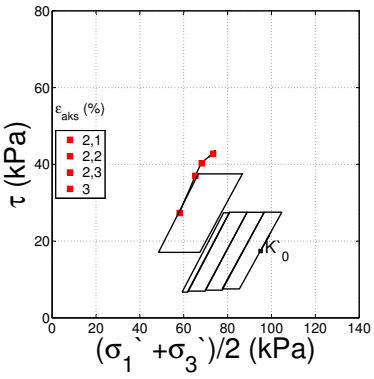
τ (kPa)
(σ1` +σ3`)/2 (kPa)
εaks (%)
2,1
2,2
2,3
3
K`0

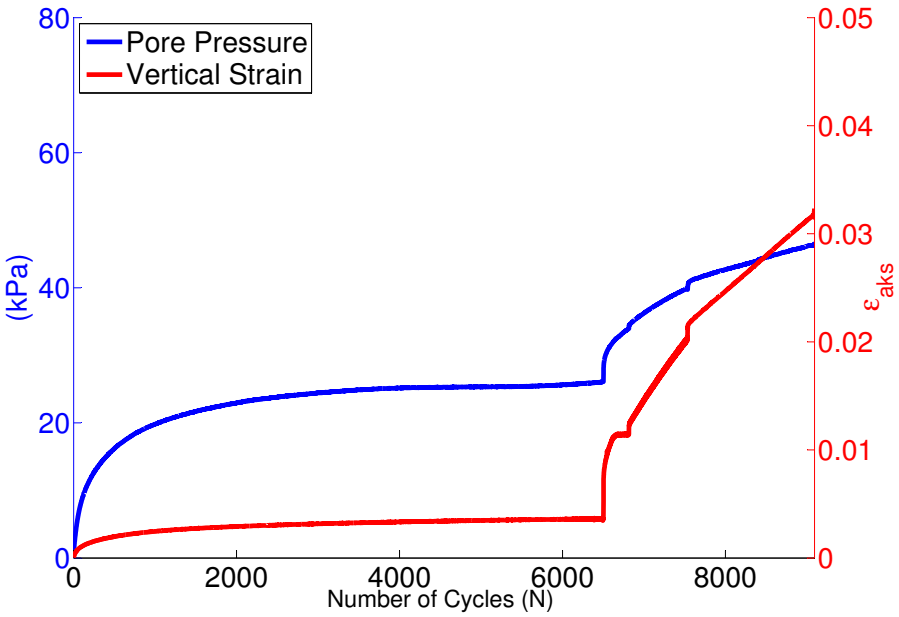
Pore Pressure
Vertical Strain
(kPa)
εaks
Number of Cycles (N)

B.3 Stjørdal: Depth 10,7 meter

This test was conducted by the following steps:

- **Step 1:** Consolidated to K_0' condition (K_0'=0,7)
- **Step 2:** $\Delta\tau_{ave}$ + 23 kPa, τ_{cyc} set to ± 5 kPa. Endured for 18 h

Table B.4 shows reached values at end of consolidation

Table B.4: Consolidation values. Depth: 10,7m

σ_v' (kPa)	σ_h' (kPa)	τ_{ave} (kPa)	ϵ_{vol} (%)
114,0	79,5	17,3	3,4

Comment

The cyclic amplitude was activated 30 seconds after the extra load was added. This delay resulted that an initial 0,5 % vertical strain accumulated before the cyclic test started.

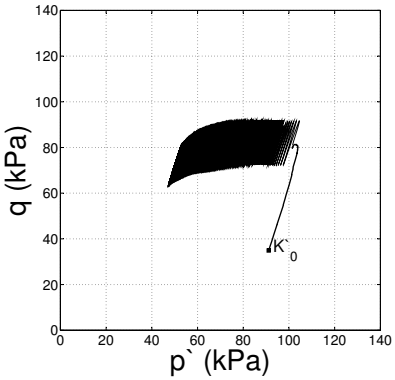
q (kPa)
p` (kPa)
K`0

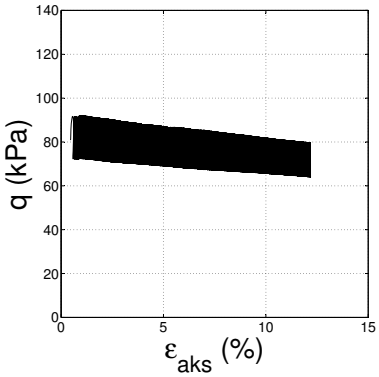
q (kPa)
εaks (%)

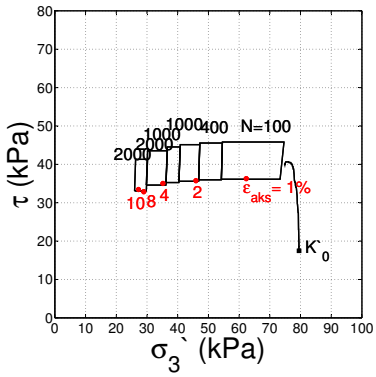
τ (kPa)
σ3` (kPa)
N=100
1000
2000
400
108
4
2
εaks= 1%
K`0

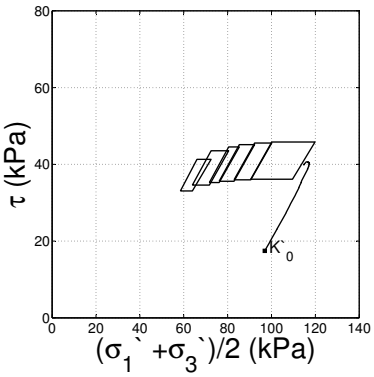
τ (kPa)
(σ1`+σ3`)/2 (kPa)
K`0

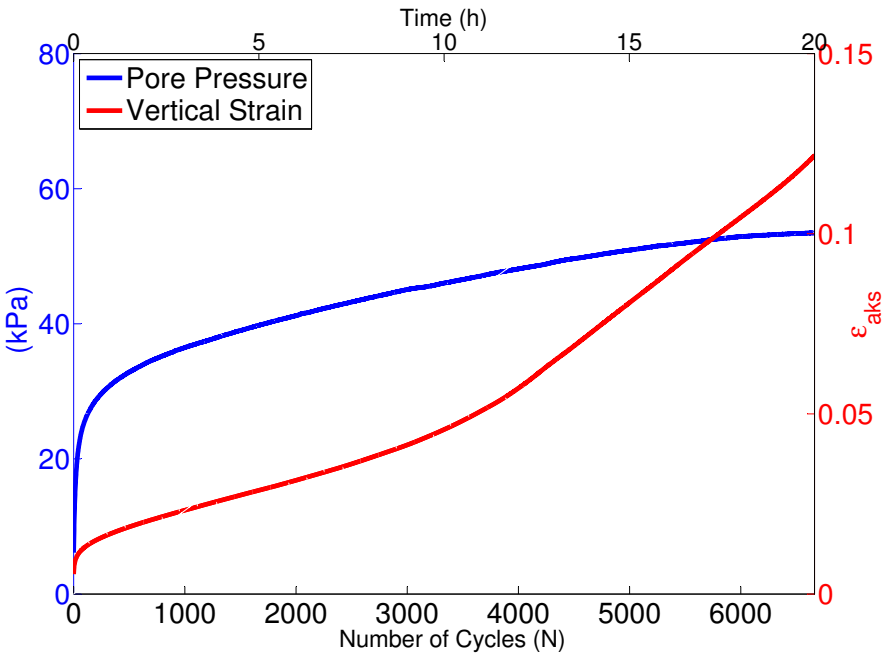
Time (h)
Pore Pressure
Vertical Strain
(kPa)
εaks
Number of Cycles (N)

B.4 Stjørdal: Depth 11,1 meter

This test was conducted by the following steps:

- **Step 1:** Consolidated to K_0' condition (K_0'=0,7)
- **Step 2:** $\Delta\tau_{ave}$ + 23 kPa, kept unchanged for 47 h.

Table B.5 shows reached values at end of consolidation

Table B.5: Consolidation values. Depth: 11,1

σ_v' (kPa)	σ_h' (kPa)	τ_{ave} (kPa)	ϵ_{vol} (%)
117,8	81,1	18,6	3,2

Comments

The added vertical load is adjusted at the start of the test.

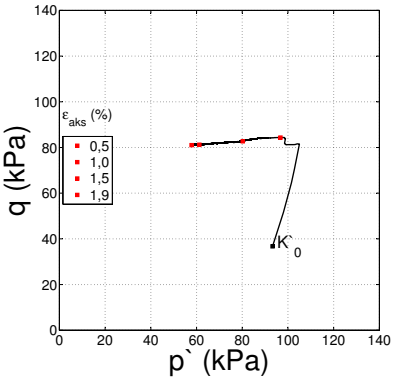
q (kPa)
p` (kPa)
ε aks (%)
0,5
1,0
1,5
1,9
K`0

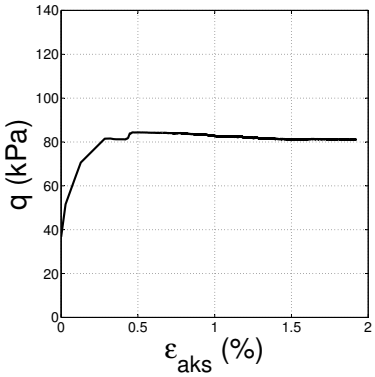
q (kPa)
ε aks (%)

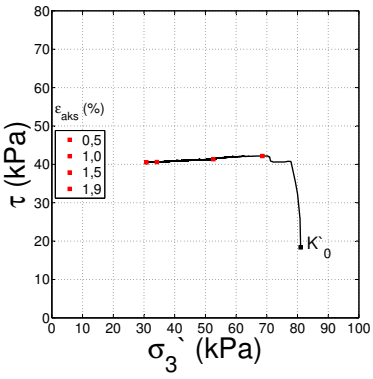
τ (kPa)
σ3` (kPa)
ε aks (%)
0,5
1,0
1,5
1,9
K`0

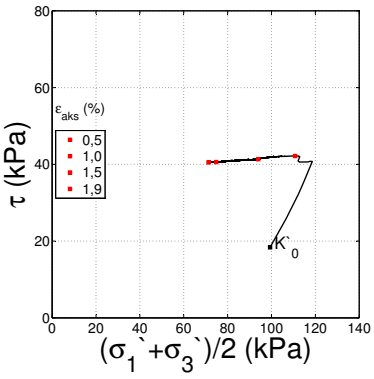
τ (kPa)
(σ1`+σ3`)/2 (kPa)
ε aks (%)
0,5
1,0
1,5
1,9
K`0

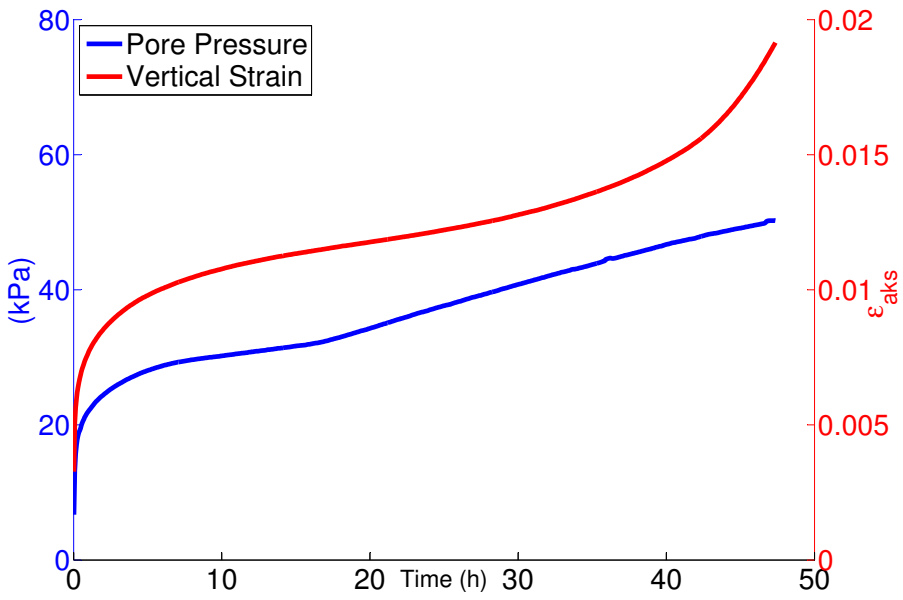
Pore Pressure
Vertical Strain
(kPa)
Time (h)
ε aks

B.5 Stjørdal: Depth 11,2 meter

This test was conducted by the following steps:

- **Step 1:** Consolidated to K_0' condition(K_0'=0,7)
- **Step 2:** $\Delta\tau_{ave}$ + 5 kPa, τ_{cyc} set ± 20 kPa. Ended after 30 min
- **Step 3:** τ_{cyc} set to ± 5 kPa. Ended after 14 h
- **Step 4:** Shear phase: Strain rate set to 1,5 %/h

Table B.6 shows reached values at end of consolidation

Table B.6: Consolidation values. Depth: 11,2m

σ_v' (kPa)	σ_h' (kPa)	τ_{ave} (kPa)	ϵ_{vol} (%)
117,6	82,7	17,5	3,2

Comments

After the first cyclic phase ended, it took 1 min to start the second phase. During this minute the pore pressure increased. That is why the last 5000 cycles starts with a lower effective stress than the end of the first cyclic phase. Almost no change in strain or pore pressure was measured for the last 5000 cycles.

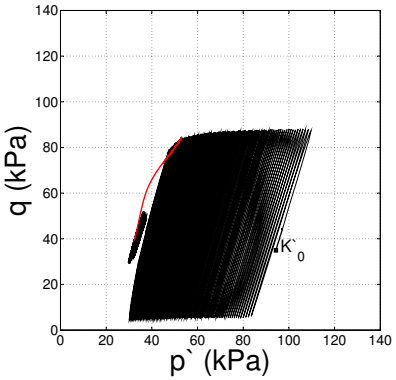
q (kPa)
p` (kPa)
K`0

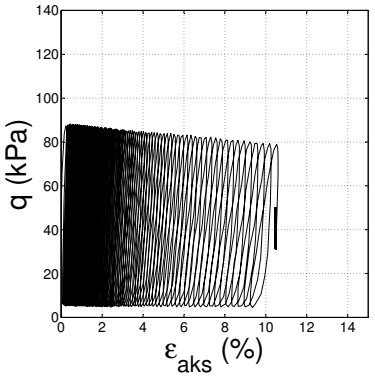
q (kPa)
εaks (%)

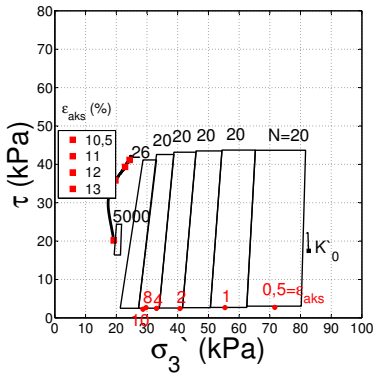
τ (kPa)
σ3` (kPa)
εaks (%)
10,5
11
12
13
N=20
5000
K`0
0,5=εaks

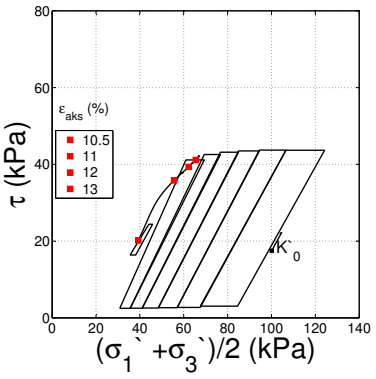
τ (kPa)
(σ1` +σ3`)/2 (kPa)
εaks (%)
10.5
11
12
13
K`0

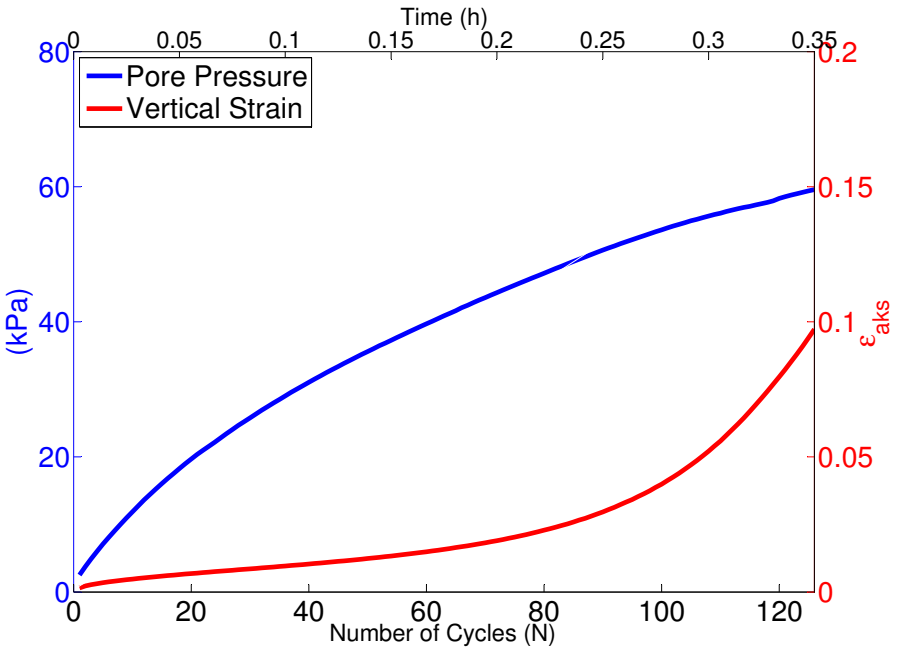
Time (h)
Pore Pressure
Vertical Strain
(kPa)
εaks
Number of Cycles (N)

B.6 Stjørdal: Depth 11,4 meter

This test was conducted by the following steps:

- **Step 1:** Consolidated to K_0' condition($K_0' = 0,7$)
- **Step 2:** Shear phase: Strain rate set to 3 %/h

Table B.7 shows reached values at end of consolidation

Table B.7: Consolidation values. Depth: 11,4m

σ_v' (kPa)	σ_h' (kPa)	τ_{ave} (kPa)	ϵ_{vol} (%)
119,3	82,6	18,4	3,1

Comments

By the pore pressure development the quality of this test may not be that good. After roughly 30 min the pore pressure flattens out, before it starts increasing again. This indicate a disturbance to the testing device, and it might be due to friction.

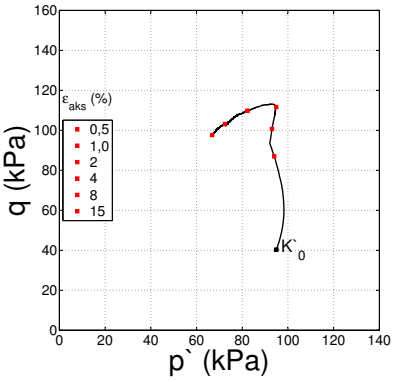
q (kPa)
p` (kPa)
ε aks (%)
0,5
1,0
2
4
8
15
K`0

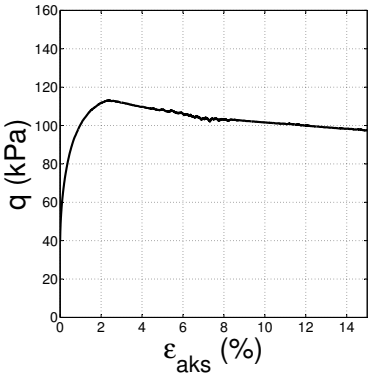
q (kPa)
ε aks (%)

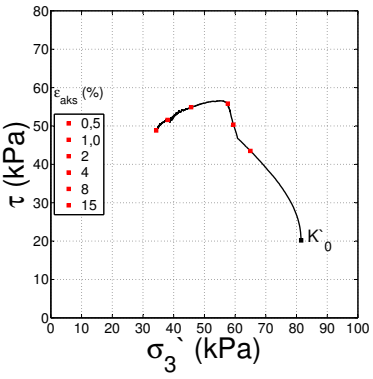
τ (kPa)
σ3` (kPa)
ε aks (%)
0,5
1,0
2
4
8
15
K`0

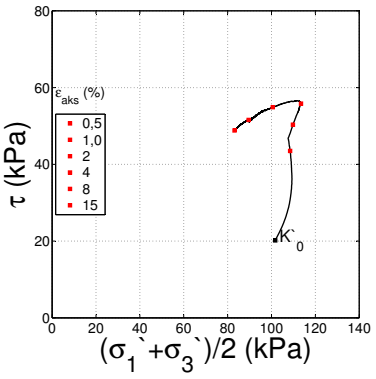
τ (kPa)
(σ1`+σ3`)/2 (kPa)
ε aks (%)
0,5
1,0
2
4
8
15
K`0

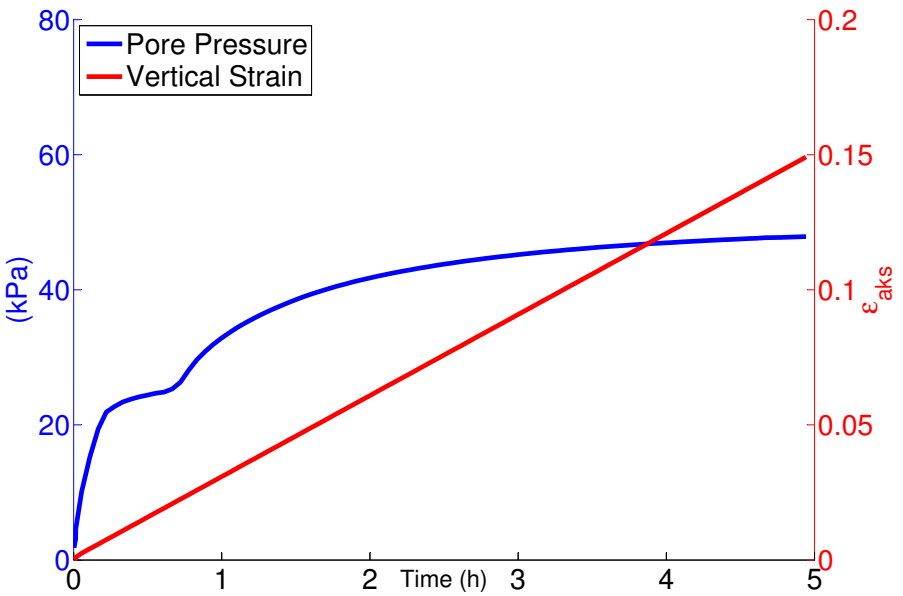
Pore Pressure
Vertical Strain
(kPa)
Time (h)
ε aks

B.7 Stjørdal: Depth 11,5 meter

This test was conducted by the following steps:

- **Step 1:** Consolidated to K_0' condition($K_0' = 0,7$)
- **Step 2:** $\Delta\tau_{ave}$ + 5 kPa, τ_{cyc} set to ±20 kPa. Step ended after roughly 30 min
- **Step 3:** Shear phase: A constant strain rate of 1,5 %/h applied. The shear phase was ended at 37,9% deformation

Table B.8 shows reached values at end of consolidation

Table B.8: Consolidation values. Depth: 11,5m

σ_v' (kPa)	σ_h' (kPa)	τ_{ave} (kPa)	ϵ_{vol} (%)
120,6	84,4	18,1	3,6

Comments

The change from dilative to contractive behavior happens at very high strains. The sample is at so large deformations that it will change properties.

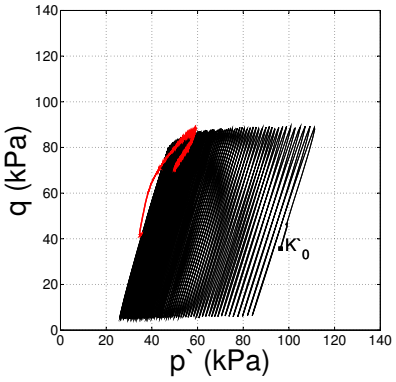
q (kPa)
p` (kPa)
K`0

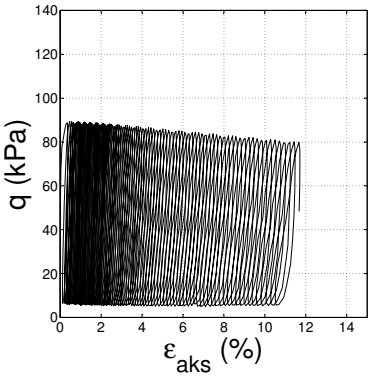
q (kPa)
εaks (%)

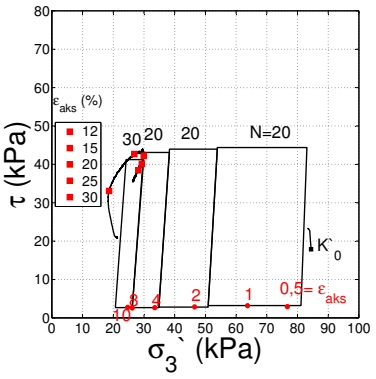
τ (kPa)
σ3` (kPa)
εaks (%)
12
15
20
25
30
30 20 20 N=20
K`0
0,5= εaks

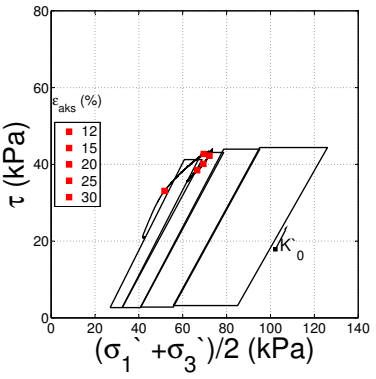
τ (kPa)
(σ1` +σ3`)/2 (kPa)
εaks (%)
12
15
20
25
30
K`0

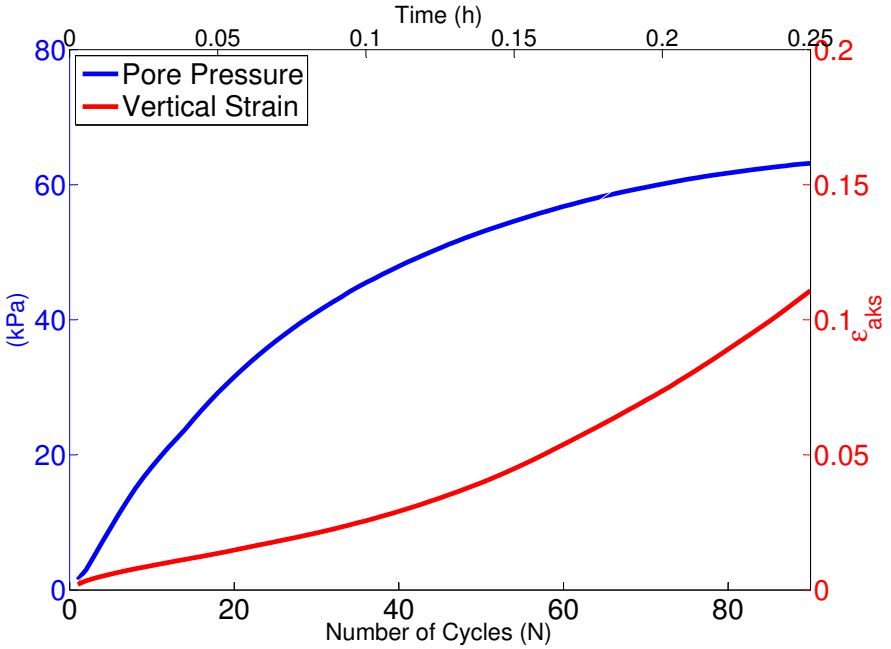
Time (h)
Pore Pressure
Vertical Strain
(kPa)
εaks
Number of Cycles (N)

B.8 Stjørdal: Depth 11,6 meter

This test was conducted with the following steps:

- **Step 1:** Consolidated to K_0' condition ($K_0' = 0,7$)
- **Step 2:** $\Delta\tau_{ave}$ + 5 kPa, ϵ_{cyc} set $\pm$75 μm. This step endured for 2 h.
- **Step 3:** Shear phase: A constant strain rate of 1,5 %/h applied. The shear phase was ended at 15 % deformation

Table B.9 shows reached values at end of consolidation

Table B.9: Consolidation values. Depth: 11,6m

σ_v' (kPa)	σ_h' (kPa)	τ_{ave} (kPa)	ϵ_{vol} (%)
122,9	82,2	20,4	5,3

Comments

Missing 45 sec of date between end of consolidation and start of cyclic phase. This resulted that the pore pressure at the start of the cyclic phase starts at 9 kPa. A long time test could possible damage the engine and is therefor not desirable. The test was therefore stopped after a 2 hours.

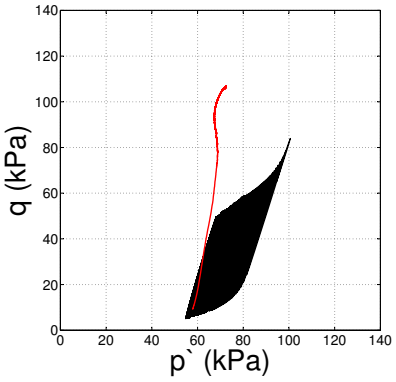
q (kPa)
p` (kPa)
0
20
40
60
80
100
120
140

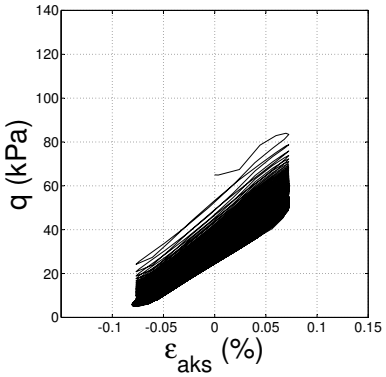
q (kPa)
ε aks (%)
-0.1
-0.05
0
0.05
0.1
0.15

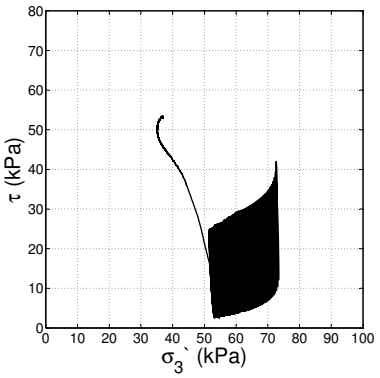
τ (kPa)
σ3` (kPa)
0
10
20
30
40
50
60
70
80
90
100

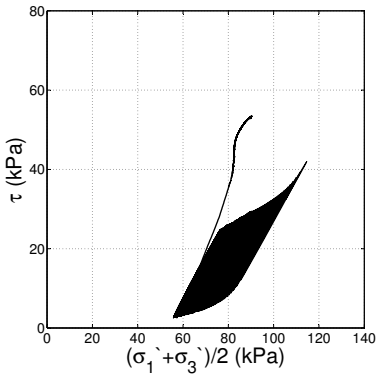
τ (kPa)
(σ1`+σ3`)/2 (kPa)

C. Cyclic Strain and Stress Development

This appendix shows the development of the cyclic pore pressure and cyclic shear strain vs. the respective average values for some of the tests in Appendix B. Table C.1 shows an overview of the tests presented.

Table C.1: Tests where cyclic pore pressure and shear strain are shown

Depth (m)	**Cyclic Amplitude** (-)
11,2	Load controlled
11,5	Load controlled
11,6	Strain controlled

The average shear stress in each section is the value at start of the test.

C.1 Stjørdal: Depth 11,2 meter

Figure C.1 shows development of strain and pore pressure from the first cyclic phase in the test from depth 11,2m. The amplitude and initial shear stress are presented in Table C.2.

Table C.2: Depth 11,2: Initial shear stress and load amplitude

τ_{ave}	τ_{cyc}
22,5 kPa	± 20 kPa

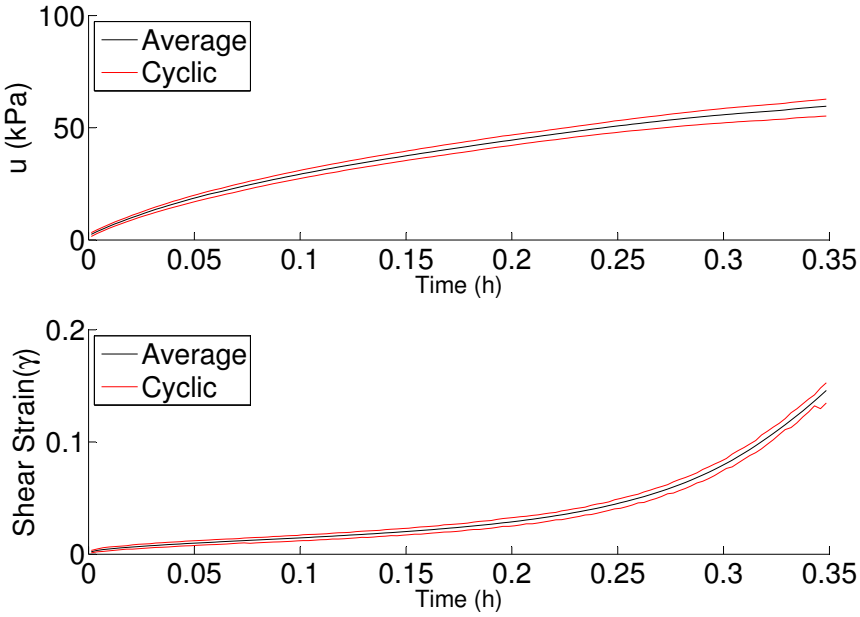

Figure C.1: Depth 11,2: Cyclic pore pressure and shear strain vs. average values

C.2 Stjørdal: Depth 11,5 meter

Figure C.2 shows development of strain and pore pressure from the cyclic phase in the test from depth 11,5m. The amplitude and initial shear stress are presented in Table C.3.

Table C.3: Depth 11,5: Initial shear stress and load amplitude

τ_{ave}	τ_{cyc}
23,1 kPa	± 20 kPa

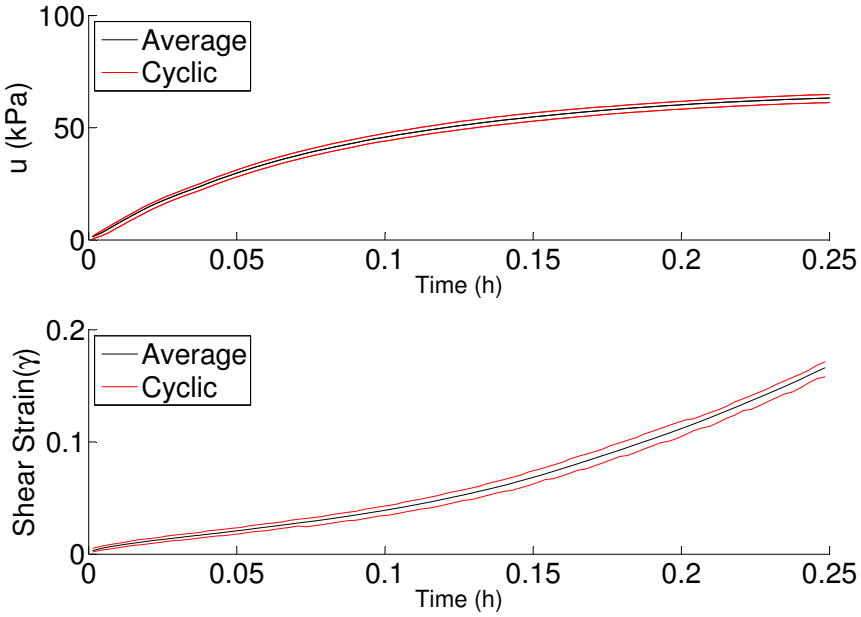

Figure C.2: Depth 11,5: Cyclic pore pressure and shear strain vs. average values

C.3 Stjørdal: Depth 11,6 meter

Figure C.3 shows development of strain and pore pressure from the cyclic phase in the test from depth 11,6m. The amplitude and initial shear stress are presented in Table C.4.

Table C.4: Depth 11,6: Shear stress and strain amplitude

τ_{ave}	ϵ_{cyc}
25,4 kPa	$\pm$ 75 μm

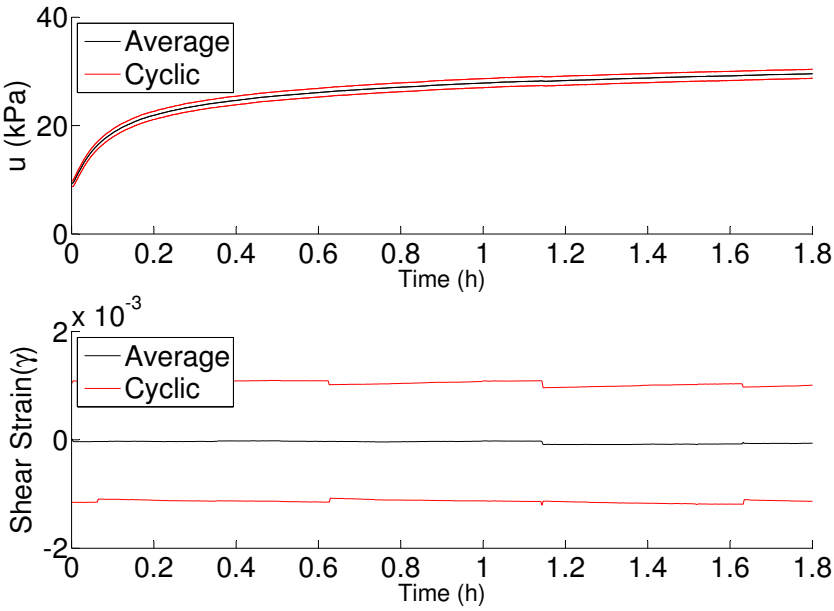

Figure C.3: Depth 11,6: Cyclic pore pressure and shear strain vs. average values

D. Validation

D.1 Triaxial Shear Test

Calculated results by simulating a triaxial shear test for two different load situations are presented, each with different set of parameters used. Results from the user-defined scripts are compared to hand calculated values and/or the Cam Clay Model implemented in PLAXIS.

The calculated values are obtained using Soil Test in PLAXIS 2D 2012. The Soil Test option allows for an easy simulation of a triaxial shear test. By this option the total response from the soil is described by the calculated value at one Gauss point. Failure is for all cases defined at 15 % strain

Two user-defined scripts are validated: The Cam Clay Model w/ Degradation(CCMD) and the Multi Parameter Script(MPS). The CCMD is used as a soil model in the MPS.

Two different scenarios are presented. One highly overconsolidated(OC) and the other is slightly overconsolidated refered to as NC.

Table D.1: Scenarios used for validation of used-defined models

Scenarios	$\boldsymbol{\kappa}$ (-)	$\boldsymbol{\lambda}$ (-)	**G** (kPa)	$\boldsymbol{e_0}$ (-)	**M** (-)	$\boldsymbol{p'_{ini}}$ (kPa)	$\boldsymbol{p'_0}$ (kPa)	**OCR** (-)
NC	0,04	0,2	2000	0,5	1,0	240	300	1,25
OC	0,06	0,3	2700	1,0	1,5	60	200	3,33

D.1.1 Cam Clay Model w/ Degradation

Validation of the user-defined Cam Clay Model is done by comparing the result from the two different scenarios presented in Table D.1 with hand calculations and the Modified Cam Clay Model (MCCM) implemented in PLAXIS.

The degradation of the clay structure is not taken into account in this comparison ($x_0 = 0$).

The results are presented in Table D.2.

Table D.2: Results Cam Clay w/ Degradation

		By Hand	**MCCM**	**CCMD**
NC	$q_f(kPa$	165,0	139,5	165,6
	$u_f(kPa)$	135,0	147,1	129,5
OC	$q_f(kPa)$	135,0	100,6	137,4
	$u_f(kPa)$	15,0	26,5	14,2

The hand calculated values and the values from CCMD have a good match. On the other hand, the values obtained using the implemented model in PLAXIS deviates from these two. It is confirmed by Plaxis Support team that there is some errors in the Cam Clay implemented in PLAXIS 2D 2012. The results from the MCCM is therefore neglected.

The shear stiffness(G) is not taken into account in the hand calculations. Regardless of the shear stiffness the deviatoric stress(q_f) at failure will not largely be affected by this value.

D.1.2 Multi Parameter Script

An assumption made in the Multi Parameter Script(MPS) is that the initial stresses at each Gauss point is divided equally to all elements included into the model.

An initial condition with a stress path is shown in Figure D.1a. This problem is divided into two elements, both applied with the same set of material parameters as the initial condition. The new situation is shown in Figure D.1b.

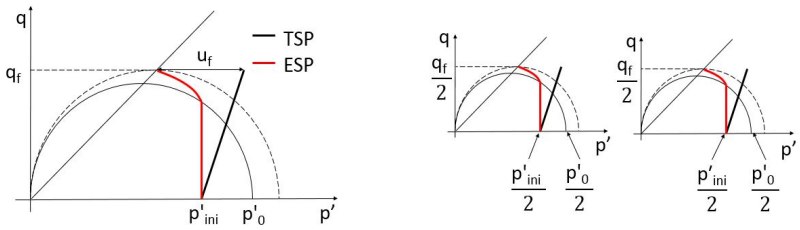

(a) Initial stress state (b) Two models

Figure D.1: An isotropic stress state described by two independent models

To see how this assumption would affect the results and to see if the MPS contained any errors, results from the MPS are compared to hand calculated values. The CCMD model is used as the soil model in the MPS. The result are summed in Table D.3. The initial condition is divided into two and three equally elements.Pore pressure(u_f) and deviatoric stress(q_f) at failure are calculated. The parameters used in the calculations are given in Table D.1.

Table D.3: Results MPS

		By Hand			MPS		
		n=1	**n=2**	**n=3**	**n=1**	**n=2**	**n=3**
NC	$q_f(kPa)$	165,6	166,1	166,7	165,7	165,9	166,7
	$u_f(kPa)$	129,5	129,1	128,8	129,6	129,2	128,2
OC	$q_f(kPa)$	136,6	138,1	139,9	136,3	138,1	140,1
	$u_f(kPa)$	14,7	14,1	13,5	14,5	14,1	14,1

D.1.3 Hand calculations

The stress path based on the different scenarios presented in Table D.1 when loaded to failure are shown in Figure D.2a and D.2b.

As for case when the initial stresses are divided equally to n number of elements, the shape of each stress path will be equal as the one presented in Figure D.2a and D.2b. But the initial stresses and preconsolidation have an lower value.

The maximum capacity at failure, for the two cases, may then be calculated by the expression:

$$\begin{aligned}\Delta V_{AF} &= \Delta V_{AB} + \Delta V_{BC} + \Delta V_{CF} = 0 \\ &= -\kappa * \ln(\frac{p'_B}{p'_A}) - \lambda * \ln(\frac{p'_C}{p'_B}) - \kappa * \ln(\frac{p'_F}{p'_C}) = 0 \end{aligned} \tag{D.1}$$

The stress at point B is equal to the preconsolidation stress. And the stress at failure is half the value at point C. Eq. (D.1) may then be solved with respect to p'_C and the effective mean stress at failure(p'_F) may be found. The deviatoric stress at failure is found from the following expression:

$$q_{maks} = q_F = (M * \frac{p'_C}{2}) \tag{D.2}$$

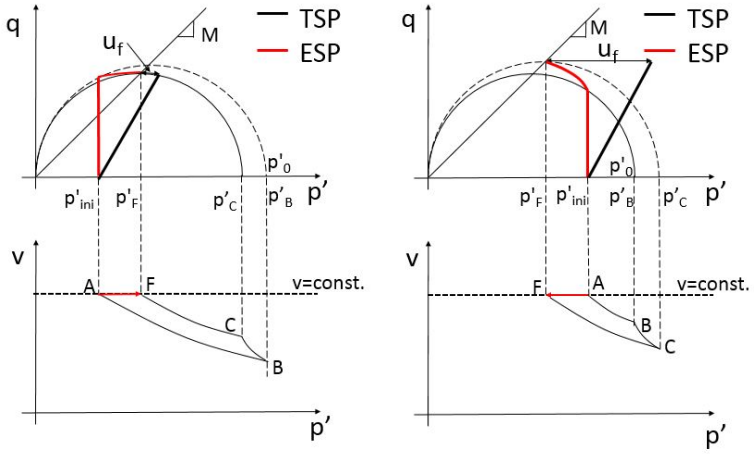

(a) OC (b) NC

Figure D.2: Stress path, undrained Cam Clay

The pore pressure is calculated as the difference between the TSP and the ESP at failure. In a trixial compression test the total stress path is equal to 1:3 in a p'-q diagram.

The results from the hand calculations are presented in Section D.1.1 and D.1.2.

D.2 Cyclic Triaxial Test

D.2.1 Model

Simulation of a triaxial test model in PLAXIS 2D 2012 is presented in Figure D.3

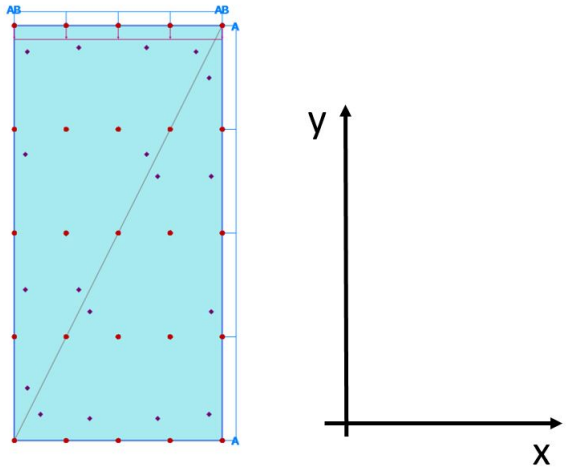

Figure D.3: Triaxial device in PLAXIS and system of axis

The model used consists of two elements. Each element have 15 nodal points, indicated by red dots. There are 12 Gauss points at each element. The triaxial test is modeled as an axissymmetric model, because the cross section of the test sample is assumed uniform and circular.

The system is massless, no absorbent boundaries has been chosen.

D.2.2 Further evaluation of cyclic results

Parameters used to obtain an increased plastic strain, by lower the shear modulus equally in all groups, are presented in Table D.4.

Table D.4: Lower the shear modulus equal in all sets

	κ (-)	λ (-)	G (kPa)	e_0 (-)	M (-)	OCR (-)	x_0 (-)	a_p (-)	a_q (-)
Set 1	0,06	0,4	2500	0,7	0,6	1,1	5	4,5	2,0
Set 2	0,05	0,5	2900	0,5	0,4	1,2	4	4,5	2,0
Set 3	0,06	0,3	1900	0,4	1,2	1,4	5	4,0	1,5

The material parameters used when the shear modulus was distributed according to strength are given in Table D.5.

Table D.5: Distribution of shear modulus according to strength

	κ (-)	λ (-)	G (kPa)	e_0 (-)	M (-)	OCR (-)	x_0 (-)	a_p (-)	a_q (-)
Set 1	0,02	0,70	4000	0,3	0,2	1,3	4,0	7,0	4,5
Set 2	0,06	0,50	4000	0,5	0,3	1,2	4,0	4,5	2,0
Set 3	0,03	0,70	2500	0,3	0,4	1,0	5,0	7,0	3,5
Set 4	0,02	0,70	2500	0,1	0,5	1.1	5,0	7,0	3,5
Set 5	0,06	0,40	2500	0,7	0.5	1.1	5,0	4,5	2,0
Set 6	0,05	0,50	2900	0,5	0.9	1.2	4,0	4,5	2,0
Set 7	0,06	0,3	1900	0,4	1,2	1,4	5,0	4,0	1,5
Set 8	0,03	0,7	1200	0,2	0,9	1,2	4,0	7,0	4,5
Set 9	0,03	0,7	950	0,2	1,1	1,2	4,0	7,0	4,5
Set 10	0,04	0,6	950	0,3	1,4	1,3	4,0	7,0	4,5

Figure D.4 and D.5 shows how the applied load changes when the shear modulus was distributed according to strength of the material (results from Section 7.2).

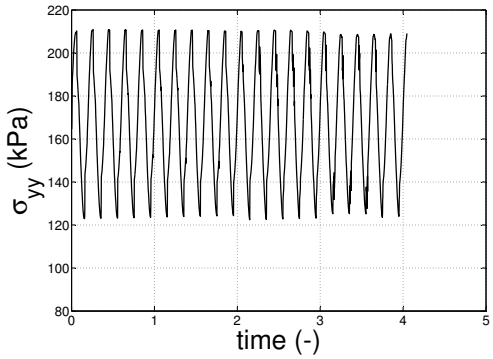

Figure D.4: Change in vertical load, shear modulus distributed according to strength of the parameters

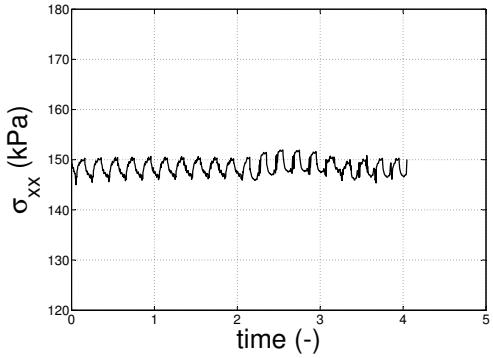

Figure D.5: Change in horizontal load, shear modulus distributed according to strength of the parameters

E. User Manual MPS

The MPS enables the user to divide an initial stress state into groups and use a chosen soil model to calculate the response of each of these groups. All groups are coupled together in parallel.

The Multi Parameter Script (MPS) is designed to work with any user-defined material model that follows the PLAXIS Subroutine setup. The setup for user-defined soil models in PLAXIS may be found in the PLAXIS Material Manual. The setup and syntax at each user-defined material model may differ, which may make some modifications to the MPS necessary.

E.1 Modifications

All modifications are done in MPS.for file(text file). After the MPS.for file has been edited it must be compiled to a .dll file, e.g. MPS.dll. To make the MPS available in PLAXIS the MPS.dll file has to be copied to the right destination folder.

Possible adjustments that may be done in the MPS or the included material model are:

State Parameter: At the start of each new calculation phase, the subroutine is called with IDTask 1. If the MPS has been used in the previous calculation phase , IDTask 1 should not be initialized. This is controlled by selecting a random State Parameter, which if already initialized is not equal to a known value.

Rename: The main subroutine for the include material model has to be renamed to match with the proper call name in the MPS.

nProps: nProps is the number of material parameters in the included soil model. nProps is defined at the start of the script.

nStat: Number of total state parameters (nStat) can be calculated from equation (E.1).

$$nStat = n * (nStati + 6) \tag{E.1}$$

where n is equal to number of material sets included and nStati are the number of state parameters specific for the included material model. The number 6 reflects the number of stress components.

The user has to check if the stresses are implemented into the state variable vector in the included soil model. If nStati contains the stresses the number 6 should not be added in Eq. (E.1).

If the stresses are included into the state variable vector, the user have to evaluated the order the state variables should be written. The two alternatives are before or after the stresses.

The attached Fortran code in Appendix F, is written with the stress vector include into the beginning of the state variable vector. The stresses and state variables for each group are calculated and included into the global state variable vector. nStat is defined under "IDTask 4", in the MPS.

Define Input Data: If the soil parameters in a user-defined model are implemented via the PLAXIS Calculation window, number of parameters are limited to a number of 50. If the parameters are included by a separate text file, the number is unlimited. The MPS is designed to read in the material parameters from a .txt file. Each set of parameters should be written on separate rows, separated by a single space. Decimal points are

given as "." not ",". The parameters should be written in the same order as they are defined in the material model.

E.2 Software

Text Editor

Almost all text editor programs may be used, as long as the file is saved with the right encoding (ANSI). For this thesis Notepad ++ is chosen because the program is helpful with the FORTRAN coding. It can be found at notepad-plus-plus.org. The script has been written in fixed format.

Compiler

As long as i follows the correct syntax the user can choose between any programming language. But because of the compiling to the .dll files it is recommended that Fortran is used. A free Fortan compiler may be found at www.mingw.org.

FEM program

PLAXIS 2012 must be used since all codes are based on this the syntax for this program. It is available at www.plaxis.nl. Newer versions of PLAXIS may also work as long as the subroutine setup is kept unchanged.

F. Fortran Source Code

F.1 Iwan model, parallel coupling

The presented setup divides a stress state into seven groups. All groups are combined by parallel coupling. As the script is written it fits with the Cam Clay Model made by Jon A. Rønningen.

```
1       Subroutine User_Mod ( IDTask, iMod, IsUndr,
2      *                      iStep, iTer, iEl, Int,
3      *                      X, Y, Z,
4      *                      Time0, dTime,
5      *                      Props, Sig0, Swp0, StVar0,
6      *                      dEps, D, BulkW,
7      *                      Sig, Swp, StVar, ipl,
8      *                      nStat, NonSym, iStrsDep, iTimeDep,
9      *                      iTang,iPrjDir, iPrjLen, iAbort )
10
11 !
12 !  Depending on IDTask, 1 : Initialize state variables
13 !                       2 : calculate stresses,
14 !                       3 : calculate material stiffness matrix
15 !                       4 : return number of state variables
16 !                       5 : inquire matrix properties
17 !                           return switch for non-symmetric D-
       matrix
18 !                           stress/time dependent matrix
19 !                       6 : calculate elastic material
       stiffness matrix
20 ! Arguments:
21 !           I/O  Type
22 !  IDTask   I    I     : see above
23 !  iMod     I    I     : model number (1..10)
24 !  IsUndr   I    I     : =1 for undrained, 0 otherwise
25 !  iStep    I    I     : Global step number
```

```
!   iter       I    I      : Global iteration number
!   iel        I    I      : Global element number
!   Int        I    I      : Global integration point number
!   X          I    R      : X-Position of integration point
!   Y          I    R      : Y-Position of integration point
!   Z          I    R      : Z-Position of integration point
!   Time0      I    R      : Time at start of step
!   dTime      I    R      : Time increment
!   Props      I    R()    : List with model parameters
!   Sig0       I    R()    : Stresses at start of step
!   Swp0       I    R      : Excess pore pressure start of step
!   StVar0     I    R()    : State variable at start of step
!   dEps       I    R()    : Strain increment
!   D          I/O  R(,)   : Material stiffness matrix
!   BulkW      I/O  R      : Bulkmodulus for water (undrained only)
!   Sig        O    R()    : Resulting stresses
!   Swp        O    R      : Resulting excess pore pressure
!   StVar      O    R()    : Resulting values state variables
!   ipl        O    I      : Plasticity indicator
!   nStat      O    I      : Number of state variables
!   NonSym     O    I      : Non-Symmetric D-matrix ?
!   iStrsDep   O    I      : =1 for stress dependent D-matrix
!   iTimeDep   O    I      : =1 for time dependent D-matrix
!   iTang      O    I      : =1 for tangent matrix
!   iAbort     O    I      : =1 to force stopping of calculation

      IMPLICIT NONE

!        Subroutine arguments
      Integer :: IDTask, iMod, IsUndr, iStep, iter, iel, Int
      Real(8) :: X,Y,Z,Time0,dTime, Sig0(6), Props1(100)
      Real(8) :: Props(100), Propsi(100), Propsii(100)
      Real(8) :: Sig0i(6), Swp0, Swp0i, StVar0(nStat)
      Real(8) :: dEps(6), D(6,6), Di(6,6), Dii(6,6), BulkW
      Real(8) :: Sig(6), Sigi(6), Swp, Swpi, StVar(nStat)
      Real(8) :: Sig0tot1(1:500), StVar0i(nStat),, Bulkwi
      Real(8) :: StVari(nStat)
      Integer :: ipl, NonSym,iStrsDep,iTimeDep,iTang,iAbort
      Integer :: nStat, nStati=3, nProps, dummyvar=125d0
      Integer :: iPrjDir(iPrjLen),iPrjLen

```

```
67  ! User defined parameters
68        Integer :: iounit = 0, i, ios, j, k
69        Save iounit
70        Character(255) :: PrjDir
71
72  ! Set all internal variables to zero
73        Di(1:6,1:6)=0d0
74        Dii(1:6,1:6)=0d0
75        BulkWi=0d0
76        Swp0i=0d0
77        Swpi=0d0
78        Sig0i(1:6)=0d0
79        Sigi(1:6)=0d0
80        StVar0i(1:nStat)=0d0
81        StVari(1:nStat)= 0d0
82        Propsi(1:100)=0d0
83        Sig0tot1(1:500)=0d0
84
85  ! Number of material properties in the soil model
86        nProps=9
87
88  ! Read in parameters from file
89        IF (dummyvar .eq. 125d0) then
90        Call properties(Props1,nProps,nStati,Props)
91            dummyvar=1
92        END IF
93
94  !IDTask 1: Initialize state variables
95        IF (IDTask .EQ. 1) THEN ! CASE ( 1)
96  ! Skip IDTaks 1 if stresses and state variable already are
      initialized
97
98          If (StVar0(7) .eq. 0d0) then
99
100           Call stressdestri(nStat,nStati,Props,Sig0,Sig0tot1)
101
102           DO i=1,nStat/(nStati+6)
103           Propsi(1:nProps) =Props(nProps*i-(nProps-1):nProps*i)
104           Sig0i(1:6) = Sig0tot1((i-1)*6+1:(i-1)*6+6)
105
106           Do k=1,nStati
```

```
107                 StVar0i((i-1)*(nStati+6)+(k+6)) = 0d0
108           End Do
109
110         Call mcc ( IDTask, iMod, IsUndr,
111      *                       iStep, iTer, iEl, Int,
112      *                       X, Y, Z,
113      *                       Time0, dTime,
114      *                       Propsi, Sig0i, Swp0, StVar0i,
115      *                       dEps, Di, BulkWi,
116      *                       Sig, Swp, StVar, ipl,
117      *                       nStati, NonSym, iStrsDep, iTimeDep,
118      *                       iTang,iPrjDir, iPrjLen, iAbort )
119           do k=1,nStati
120                StVar0((i-1)*(nStati+6)+(k+6)) = StVar0i((k+6))
121           end do
122             StVar0((i-1)*(6+nStati)+(1):(i-1)*(6+nStati)+(6))
123      *                                          = Sig0i(1:6)
124
125           End DO
126         End if
127       END IF
128
129  !IDTask 2: Calculate constitutive stresses
130       IF (IDTask .EQ. 2) THEN
131           Sig(1:6)=0d0
132         DO i=1,nStat/(nStati+6)
133                Propsi(1:nProps) =Props(nProps*i-(nProps-1):
                       nProps*i)
134           Do k=1,nStati
135                StVar0i((k+6))= StVar0((i-1)*(nStati+6)+(k+6))
136           End Do
137                Sig0i(1:6) = StVar0((i-1)*(nStati+6)+(1):
138      *                                  (i-1)*(nStati+6)+(6))
139
140                  ! Stiffness matrix(Dii) for calculating
                         stresses
141         Call mcc ( 3, iMod, IsUndr,
142      *                       iStep, iTer, iEl, Int,
143      *                       X, Y, Z,
144      *                       Time0, dTime,
145      *                       Propsi, Sig0i, Swp0, StVar0i,
```

```
146       *                           dEps, Dii, BulkWi,
147       *                           Sigi, Swp, StVari, ipl,
148       *                           nStati, NonSym, iStrsDep, iTimeDep,
149       *                           iTang,iPrjDir, iPrjLen, iAbort )
150
151
152           Call mcc ( IDTask, iMod, IsUndr,
153       *                           iStep, iTer, iEl, Int,
154       *                           X, Y, Z,
155       *                           Time0, dTime,
156       *                           Propsi, Sig0i, Swp0, StVar0i,
157       *                           dEps, Dii, BulkWi,
158       *                           Sigi, Swp, StVari, ipl,
159       *                           nStati, NonSym, iStrsDep, iTimeDep,
160       *                           iTang,iPrjDir, iPrjLen, iAbort )
161             do k=1,nStati
162                   StVar((i-1)*(nStati+6)+(k+6)) = StVari((k+6))
163             end do
164                   StVar((i-1)*(6+nStati)+(1):
165       *                                       (i-1)*(6+nStati)+(6))=
            Sigi(1:6)
166                   Sig(1:6) = Sig(1:6)+Sigi(1:6)
167           END DO
168           If (isundr .eq. 1) Then
169                   swp = swp0 + BulkW * (dEps(1) + dEps(2) + dEps
                        (3))
170                   !dEpsV = 0
171           End If
172
173         END IF
174
175   !IDTask 3,6: Calculate effective/elastic D-matrix
176         IF (IDTask .EQ. 3 .OR. IDTask .EQ. 6) THEN
177
178                   D(1:6,1:6)=0d0
179                   BulkW=0d0
180
181           Do i=1,nStat/(nStati+6)
182                   Propsi(1:nProps) =Props(nProps*i-(nProps-1):
                        nProps*i)
183             Do k=1,nStati
```

```
184                 StVar0i((k+6)) = StVar0((i-1)*(nStati+6)+(k+6))
185               End Do
186
187                 Sig0i(1:6)
188       *= StVar0((i-1)*(6+nStati)+1:(i-1)*(6+nStati)+6)
189           Call mcc ( IDTask, iMod, IsUndr,
190       *                        iStep, iTer, iEl, Int,
191       *                        X, Y, Z,
192       *                        Time0, dTime,
193       *                        Propsi, Sig0i, Swp0, StVar0i,
194       *                        dEps, Di, BulkWi,
195       *                        Sig, Swp, StVar, ipl,
196       *                        nStati, NonSym, iStrsDep, iTimeDep,
197       *                        iTang,iPrjDir, iPrjLen, iAbort )
198    ! Stiffness
199                 D(1:6,1:6)= Di(1:6,1:6)+ D(1:6,1:6)
200   !Bulk Stiffness
201                 BulkW =BulkWi+BulkW
202
203           End do
204         END IF
205
206   !IDTask 4: Set number of state parameters
207         IF (IDTask .EQ. 4) THEN
208             nStat = 63
209         END IF
210
211   !IDTask 5: Define matrix type
212         IF (IDTask .EQ. 5) THEN
213             NonSym = 0          ! 1 for non-symmetric D-matrix
214             iStrsDep = 1        ! 1 for stress dependent D-matrix
215             iTang = 0           ! 1 for tangent D-matrix
216             iTimeDep = 0        ! 1 for time dependent D-matrix
217         END IF
218
219
220
221         END SUBROUTINE User_Mod
222   ! Soil Model
223         include 'usrmod.for'
224   ! Parameters
```

```
225       include 'data.for'
226 ! Stress Distribution
227       include 'stressdistr.for'
```

F.2 Subroutines

F.2.1 Parameters

This subroutine reads parameters from a text file. The setup presented is designed to read seven sets of parameters. Each set matches with the Cam Clay Model made by Jon A. Rønningen.

```
1  ! nStat also has to be specified in this script
2        Subroutine properties(propsi,nProps,nStati,props)
3        Real(8) :: Props(100), Propsi(100)
4        Real(8) ::  Propsii(100),Props2(100)
5        Integer :: nProps, nStat, nStati
6        Character(255) ::  data_file
7   !    Define nStat
8         nStat=63
9   !    Location of file with parameters
10        data_file = 'C:\Users\Christofer\Skole\data.txt'
11       Open( 3, File = data_file, status='old',action ='read')
12        DO i=1,nStat/(nStati+6)
13          read (3,*) Propsii(1:nProps)
14           do j=1,nProps
15                 Props2(nProps*i-(nProps-j)) = Propsii(j)
16           End do
17                Props(1:100)= Props2(1:100)
18        END DO
19        close(6)
20        END Subroutine
```

F.2.2 Stress distribution

This subroutine distributes initial stresses to all groups included into the model. It is explicitly made to match with the Cam Clay Model made by Jon A. Rønningen.

```
1
2       Subroutine stressdestri(nStat,nStati,Props,Sig0,Sig0tot)
3
4  ! Declaration of variables
5       Integer :: nStat, nStati
6       Real(8) :: Props(100),M(10), Sig0i(6),Sig0(6),Mtot,qtot
7       Real(8) :: const= 0d0,qi(10),pi, Sig0tot(500)
8       Character(255) :: PrjDir, dbg_file6
9       Integer :: i, ios, j, k,iounit = 0
10
11      qi=0d0
12      pi=0d0
13      Sig0tot(1:500)=0d0
14      Mtot=0d0
15
16
17 !   Put all M in a vector. Mi is variable # 5
18      Do i=1,nStat/(nStati+6)
19      M(i)=Props((i-1)*9+5)
20      Mtot=M(i)+Mtot
21      End do
22
23 !  Calculate total deviatoric stress
24      qtot=Sig0(2)-Sig0(1)
25
26 !  Calculate relationship constant
27      const=qtot/Mtot
28
29
30      Sig0i(1:6) = Sig0(1:6)/(nStat/(nStati+6))
31      pi=(Sig0i(1)+ Sig0i(2)+Sig0i(3))/3d0
32
33      if (qtot .GT. -1d0) then
34 ! Isotropic stress condition
```

```
35          Do i=1,nStat/(nStati+6)
36          Sig0tot((i-1)*6+1:(i-1)*6+6)=Sig0i(1:6)
37          End Do
38
39  ! Anisotropic stress condition
40          else
41
42          Do i=1,nStat/(nStati+6)
43                  qi(i)=M(i)*const
44
45          Sig0tot((i-1)*6+1:(i-1)*6+6)=Sig0i(1:6)
46
47          Sig0tot((i-1)*6+1)= (pi*3d0-qi(i))/3d0       ! sigx
48          Sig0tot((i-1)*6+2)=qi(i)+Sig0tot((i-1)*6+1) ! sigy
49          Sig0tot((i-1)*6+3)=Sig0tot((i-1)*6+1)          ! sigz
50           End Do
51
52           END IF
53
54           END Subroutine
```